BOEING SCIENTIFIC RESEARCH LABORATORIES DOCUMENT D1-82-0553

BOEING

SCIENTIFIC RESEARCH LABORATORIES



# Fatigue Crack Propagation under Programmed and Random Loads

J. Corey McMillan

Regis M. N. Pelloux



SOLID STATE PHYSICS LABORATORY JULY 1966

D1-82-0553

# FATIGUE CRACK PROPAGATION UNDER PROGRAMMED AND RANDOM LOADS

by

J. Corey McMillan
and
Regis M. N. Pelloux

July 1966

Solid State Physics Laboratory
Boeing Scientific Research Laboratories
Seattle, Washington

## ACKNOWLEDGMENTS

The work reported in this document is the result of a cooperative research program between the Boeing Scientific Research Laboratories and the Materials Technology Unit of the Commercial Airplane Division. This cooperative program was aimed at applying a more fundamental approach to the solution of the applied metallurgical and engineering problem of fatigue crack propagation.

The mechanical tests and the laboratory work were funded through the research budget of the Materials Technology Unit, Commercial Airplane Division.

The authors wish to thank S. H. Smith and W. E. Anderson for many valuable discussions, T. Porter for preparation of the computer programs, and W. C. Larson and W. D. Sump for conducting the mechanical tests.

## TABLE OF CONTENTS

BLANK PAGE

## ABSTRACT

The influence of maximum stress, stress range, and sequence of load application on the rate and mechanism of fatigue crack propagation in 2024-T3 aluminum alloy was studied by means of electron fractography. Variable amplitude loading programs were designed to provide tests under the following conditions:

1. Constant maximum stress with three different levels of stress range,
2. Constant stress range with three and four levels of maximum stress,
3. Pseudorandom load application achieved by random distribution of the load spectra defined in items (1) and (2),
4. Uniform maximum stress with peak overloads and underloads.

The macroscopic growth rates were determined on center-notched crack growth panels and the fracture surfaces were examined by electron fractography. The analyses of the influence of program loads on the rate and mechanism of fatigue crack growth were accomplished by:

1. Comparing plots of crack length *versus* measured rates of crack propagation for the different programs. The measured rates were also compared with rates calculated by a computer program.

7. Relating the count and spacing of the fatigue striations observed on the fracture surfaces to the applied load program, by means of electron fractography.

An empirical equation relating relative microscopic growth rates at a given crack length to maximum loads and load amplitudes was obtained. It was also found that the advance of a fatigue crack front takes place only during the loading part of a cycle and that in the pseudorandom load case the sequence of load application can markedly influence crack growth rate on any one cycle.

# I. INTRODUCTION

The "fail-safe" concepts used in design of aircraft structure require a basic knowledge and understanding of the fatigue crack propagation behavior of airframe materials. Although considerable progress has been made in the last twenty years[1,2,3,4,5] toward understanding fatigue crack propagation, the methods used to predict the fatigue properties of structure under program or random loads still have a low degree of reliability and confidence. In particular, the relationship between the fatigue damage created by random service loads and by programmed test loads has not yet been established. One of the main technical difficulties has been an inability to separate the fatigue damage induced by each load application in a complex load history. For instance, in a typical fatigue test the smallest crack length change measured with a 50X traveling microscope is of the order of .001", which may correspond to 100 or 1,000 load programs, or to an even larger number of mean crossings in a random load test. Even if we were to use a higher magnification microscope the surface measurements of crack length would not give us a load-crack length relationship with significantly greater resolution because of the uncertainty of the definition of the actual, subsurface crack tip position.

Fortunately, in most of the aluminum alloys used as airframe materials, the fatigue fracture surface itself shows the successive positions of the fatigue crack front with an amazing resolution. Suc-

cessive crack front positions spaced less than $1 \times 10^{-6}$ inches apart have been observed. The successive crack front positions are represented by a series of groove ridge lines on the fracture surface, and are called crack front arrest lines or simply fatigue striations. These striations were first observed with the optical microscope[6] but can best be studied with the electron microscope at magnifications ranging from 1,000 to 20,000. In the case of the 2000 and 7000 series of aluminum alloys the striations are remarkably well defined, at least for crack growth rates ranging from 1 to 1,000 μinch/cycle. At the lowest growth rates, where the need for growth rate information is greatest, nearly all of the fracture surface shows striations. At higher growth rates the percentage of fracture surface occupied by striations decreases. That is, fracture by cyclic ductile tear predominates as the crack approaches critical crack length.

The fact that the striations represent successive positions of the crack front enables us to study the mechanisms and rates of fatigue crack propagation as a function of crack length, load history, stress intensity factor, and environment. So far, most studies of fatigue fracture surfaces by electron microscopy have been limited to qualitative observations of the striation shapes and profiles, and to striation interactions with grain boundaries or second phase particles.[7] A limited amount of quantitative work has shown that for uniform cyclic loads and for crack growth rates greater than 1 to 10 μinch/cycle, there is a one-to-one correlation between striations

and load cycles.[8] Also, it has been shown that the measurements of striation spacing, which represent the microscopic rate of crack propagation, correlate very well with the macroscopic measurements of crack propagation rates.[9,10]

In recent studies at Boeing we used optical and electron fractography to study the fatigue fracture surfaces of many structural test components tested under programmed loads designed to simulate service conditions. In each case the load program could be readily related to the general topography of the fracture surface. However, the complexities of the test components and of the load spectra were such that it was not possible to make a direct correlation between each applied load and the observed striation spacings. As a consequence, we ran a number of fatigue crack propagation tests with different simplified spectra of loads. These loads were programmed in such a way as to lead to an unambiguous interpretation of the microfractographic observations.

The purpose of this research program was to achieve a better understanding of the following problems:

1. The influence of maximum load, load amplitude, and load sequence on crack propagation rates. Two basic types of load programs were studied: (a) constant maximum load with variable load amplitudes, and (b) constant load amplitude with variable maximum loads.

2. The comparison of pseudorandom loading with program loading. The two basic types of load programs defined above were

randomized and the crack growth rates were compared.

3. The occurrence of crack arrest and crack acceleration. Striations were counted and striation spacings were measured following changes of maximum loads or load amplitudes.

4. The mechanisms of fatigue cracking and striation formation. Some of the load sequences were planned to distinguish clearly between loading and unloading behavior at the crack tip.

5. The prediction of programmed or pseudorandom load crack propagation rates. Using crack growth data from constant maximum load and constant load amplitude tests, a computer program calculated the expected crack growth rates for all the programmed and random load tests. The validity of Miner's rule for crack propagation was evaluated by comparing calculated with observed growth rates.

## II. EXPERIMENTAL PROCEDURE

### Materials

The material chosen for this program was 2024-T3 aluminum alloy in the form of bare 0.160-inch gage sheet. The 2024-T3 alloy was selected because its fatigue crack growth rates are less susceptible to environmental effects such as humidity, than are alloys of the 7000 series.[11] Also, the fatigue striations of the 2024 alloy are always clearly defined and are of the ductile type.[12] Thus, they lend themselves to a detailed striation profile and spacing analysis. A number of similar tests were also conducted on aluminum alloy 7075-T6

to confirm the generality of relationships established for the 2024 alloy. The chemical composition and mechanical properties of the transverse grain direction of the 2024-T3 material used in this program are shown in Tables I and II, respectively.

Test Procedure

The test specimen used in the fatigue testing portion of the program was a 24" × 9" center-notched fracture panel, with the transverse grain direction parallel to the tensile axis. Fatigue testing was accomplished in a vertical 125 kip electrohydraulic fracture jig of Boeing design at a cyclic rate of 90 cpm.

Program and random loads were introduced by punched tape digital programming through a Boeing-designed forced closed loop, servo system, random load controller. Previous work has shown this testing system to be capable of applying loads with an absolute error of ±1 percent of the maximum programmed load for the random load case at cyclic rates up to 90 cpm. A typical load recording is shown in Figure 1.

The initial center crack (2a) was 0.5-inch with a crack root radius of .003-inch. Crack growth was monitored with a 50X traveling microscope. Specimens were normally cycled to failure. All testing was conducted in a laboratory environment. Temperature and relative humidity, recorded periodically throughout the tests, ranged from 65°F to 79°F and 17 percent to 52 percent relative humidity. The averages were approximately 70°F and 40 percent relative humidity.

TABLE I

CHEMICAL COMPOSITION

| Programs | Cu | Mg | Mn | Zn | Si | Cr | Fe | Ti | Al |
|---|---|---|---|---|---|---|---|---|---|
| P1 to P7, P11, P12 | 4.10 | 1.65 | 0.56 | <0.03 | 0.07 | <0.03 | 0.21 | <0.03 | BAl. |
| P8, P9, P10 | 4.44 | 1.56 | 0.66 | <0.05 | 0.08 | <0.01 | 0.17 | <0.03 | BAl. |

TABLE II

MECHANICAL PROPERTIES

| Programs | $F_{TU}$(psi) | $F_{TY}$(psi) | % Elong. | % RA |
|---|---|---|---|---|
| | 68,400 | 46,900 | 17.0 | 23.0 |
| P1 to P7, P11, P12 | 68,400 | 47,700 | 18.0 | 24.0 |
| | 69,000 | 48,000 | 19.5 | 26.0 |
| | 70,200 | 46,700 | 20 | 27 |
| P8, P9, P10 | 69,700 | 45,200 | 20 | 28 |
| | 70,500 | 45,100 | 19 | 26 |

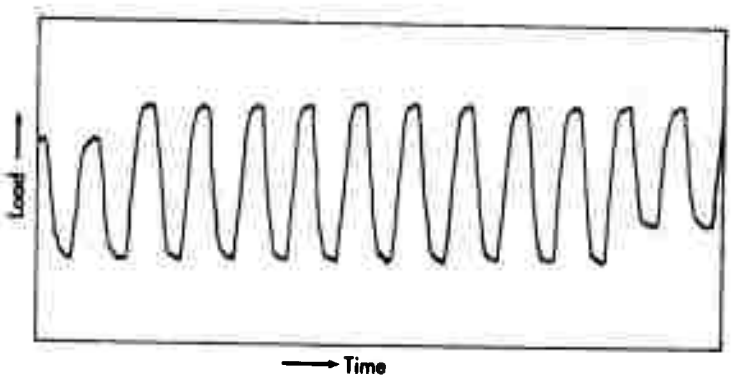


Figure 1 Typical recording of load for part of Program P13.

All the test data, crack length *versus* number of periods, are reported in Appendix I. The crack rates $\frac{d\ell}{dn}$ have been calculated as the linear average over the interval between two successive crack length readings. The crack rate obtained is assumed to be the crack rate at the middle of the crack length interval.

Standard two-stage replicating techniques were used to prepare replicas for examination with the electron microscope. The shadowing material was germanium, and in every case but one, the shadowing direction was parallel to the overall crack propagation direction. Replicas of the fracture surface were examined at average crack lengths of $2a = 0.6$, 0.9, 1.3, and 1.7 inches. The crack length corresponding to each electron micrograph was recorded with an accuracy of $\Delta a = \pm 0.02$ inch. The critical fatigue crack lengths for all specimens ranged from $2a = 6$ to 7 inches.

Test Programs

Thirteen load programs, P1 to P13, were run. Each program was broken down into spectra identified as A, B, C, and D. In each spectrum the maxima and minima of loads were numbered in sequence so that any cycle or part of a cycle could be identified and referred to without confusion. For instance, P1-A9-B1 refers to the compression part A9 to B1 of the first cycle of Spectrum B of Program P1. The cycle digits should always be read in the forward direction.

Tables IIIA and IIIB list the programs, the spectra sequence,

TABLE IIIA

PROGRAMS WITH CONSTANT MAXIMUM STRESS

(Maximum Stress Sg = 12000 psi)

| Programs | P1 | P2 | P3 | P4 | P5 |
|---|---|---|---|---|---|
| Sequence | ABC | CBA | CBA | ABCD | Random |
| Spectrum | | | | | |
| A | | | | | |
| n cycles | 9 | 9 | 6 | 12 | |
| β | 1.2 | 1.2 | 2 | 2 | |
| B | | | | | |
| n cycles | 8 | 8 | 8 | 8 | |
| β | 3 | 3 | 3 | 3 | |
| C | | | | | |
| n cycles | 7 | 7 | 10 | 20 | |
| β | 20 | 20 | 20 | 20 | |
| D | | | | | |
| n cycles | | | | 8 | |
| β | | | | 3 | |

TABLE IIIB

PROGRAMS WITH CONSTANT STRESS AMPLITUDE

(Stress Amplitude $\Delta S$ = 7000 psi)

| Programs | P6 | P7 | P8 | P9 | P10 | P11 | P12 |
|---|---|---|---|---|---|---|---|
| Sequence | ABCD | DCBA | ABC | CBA | Random | AB | AB |
| Spectrum | | | | | | | |
| A | | | | | | | |
| n cycles | 4 | 4 | 20 | 20 | | 4 | 3 |
| S max ksi | 14 | 14 | 14 | 14 | | 14 | 12 |
| $\beta$ | 2.0 | 2.0 | 2.0 | 2.0 | | 2.0 | 2.4 |
| B | | | | | | | |
| n cycles | 5 | 5 | 16 | 16 | | 20 | 21 |
| S max ksi | 12 | 12 | 12 | 12 | | 12 | 14 |
| $\beta$ | 2.4 | 2.4 | 2.4 | 2.4 | | 2.4 | 2.0 |
| C | | | | | | | |
| n cycles | 6 | 6 | 12 | 12 | | | |
| S max ksi | 10 | 10 | 10 | 10 | | | |
| $\beta$ | 3.33 | 3.33 | 3.33 | 3.33 | | | |
| D | | | | | | | |
| n cycles | 7 | 7 | | | | | |
| S max ksi | 8 | 8 | | | | | |
| $\beta$ | 11.4 | 11.4 | | | | | |

the number of cycles in each spectrum, the maximum gross area stress and stress amplitude, and $\beta$ factors $\left(\beta = \frac{S\ max}{S\ min}\right)$.

The programs are shown in Figures 2, 3, and 4. Load was approximately a sine function with time represented as triangular waves on the sketches for simplicity. Programs P1, P2, P3, P4, and P5 represent a constant maximum load with variable load amplitudes. P2 is the reverse of P1, and P3 was obtained by modifying P2 in order to obtain crack propagation with the smallest load amplitude level. P4 was made up by juxtaposing P3 and a reversed P3 to measure the influence of the sequence of load spectra. Program P5 was obtained by "randomizing" P3. The first three cycles were purposely planned with a constant $\Delta S = 11{,}400$ psi in order to have a reference marker on the microfractographs.

Programs P6, P7, P8, P9, P11, and P12 represent a constant load amplitude with variable maximum loads. P7 and P9 are the reverse, respectively, of P6 and P8. P8 and P9 were designed after it was found that P6 and P7 gave a striation profile difficult to analyze. P11 and P12 were used to identify unambiguously the cracking sequence in each cycle and also to measure the influence of overloads or underloads. P10 was obtained by "randomizing" the same number and levels of S max and S min values present in P9. Four pseudorandom programs were produced by alternately drawing a maximum and minimum stress value from separate boxes. Program P10 was then arbitrarily icked from among the four pseudorandom programs. In this paper,

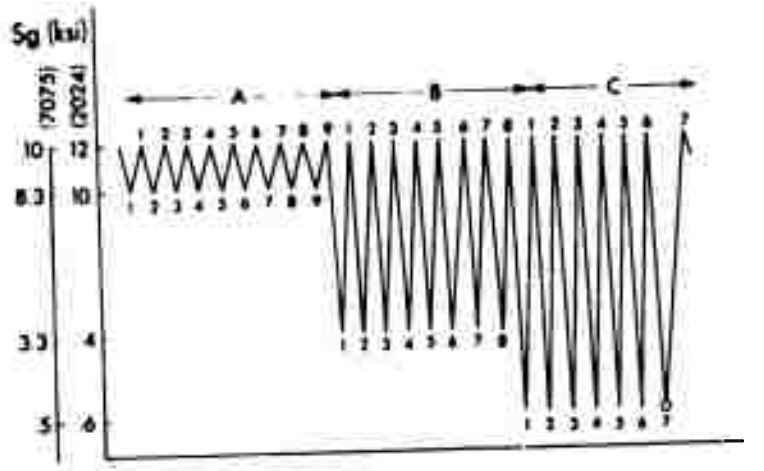


Figure 2a Program P1.

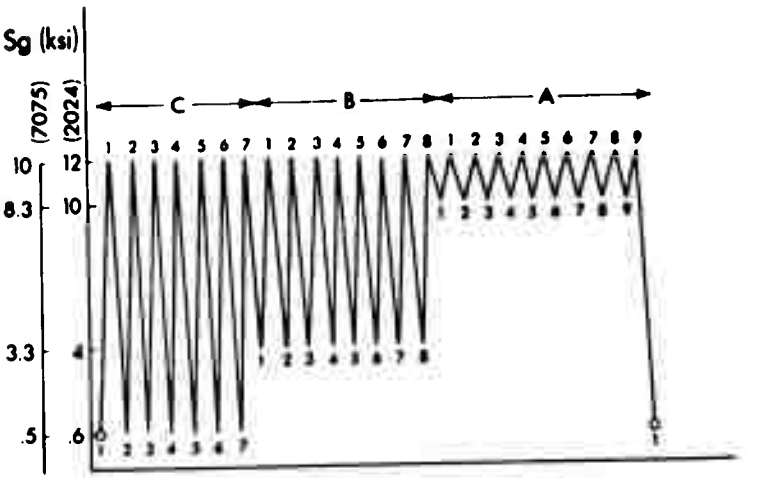


Figure 2b Program P2.

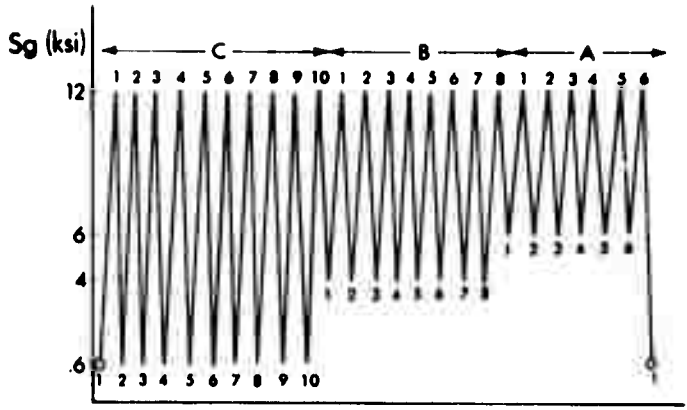


Figure 2c Program P3.

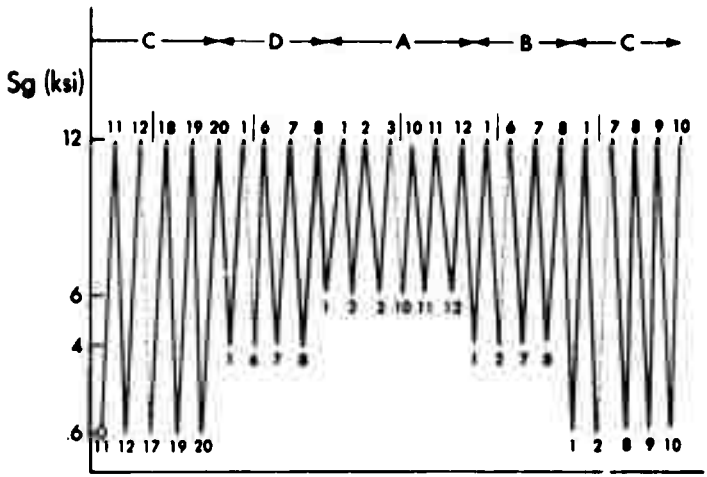


Figure 2d Program P4.

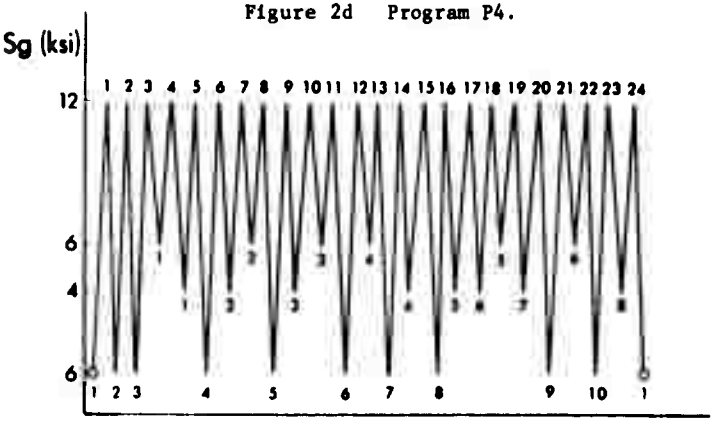


Figure 2e Program P5.

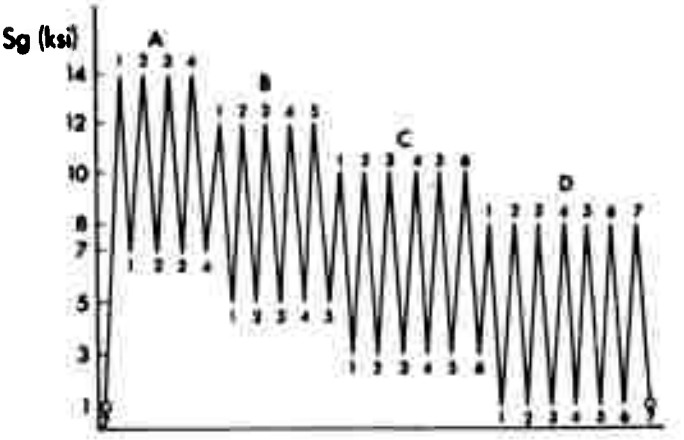


Figure 3a Program P6.

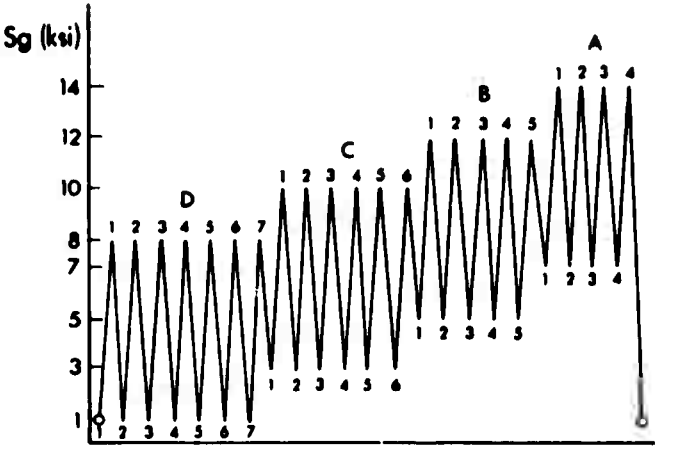


Figure 3b Program P7.

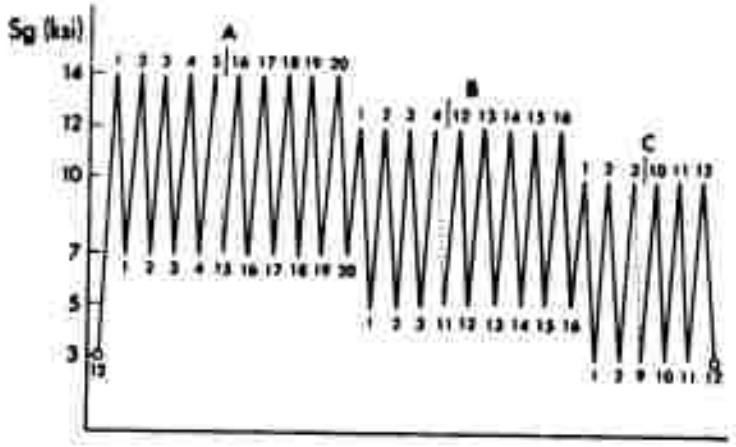


Figure 3c Program P8.

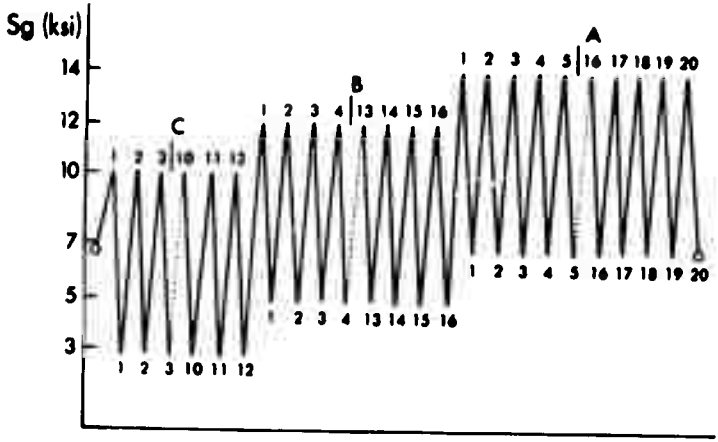


Figure 3d Program P9.

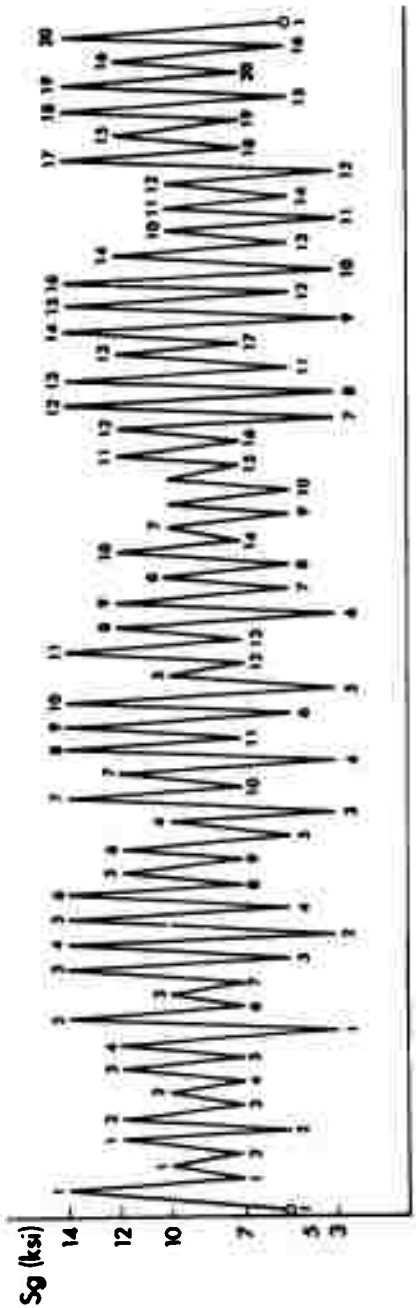


Figure 3e Program P10.

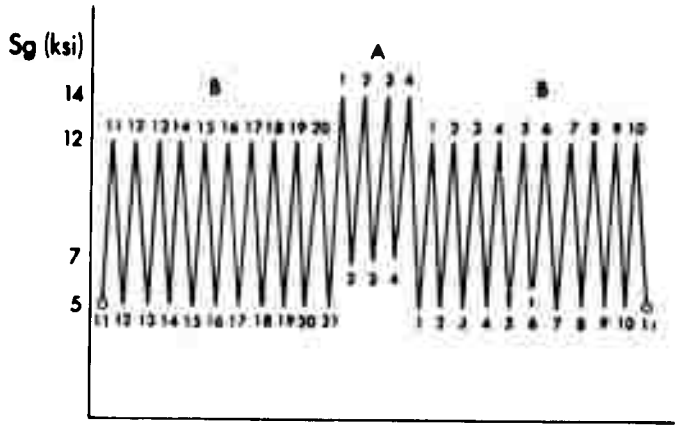


Figure 4a Program P11.

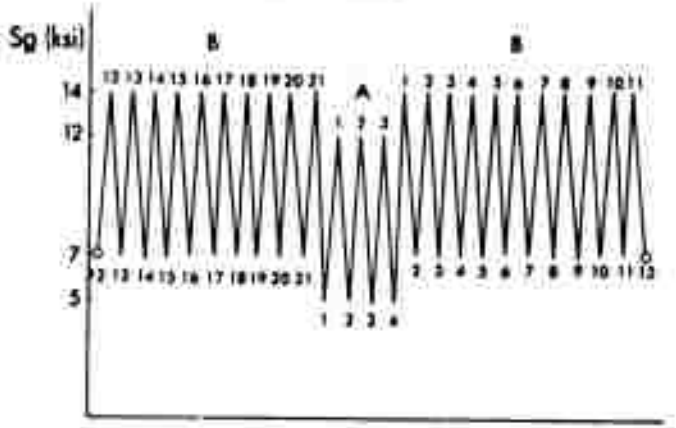


Figure 4b Program P12.

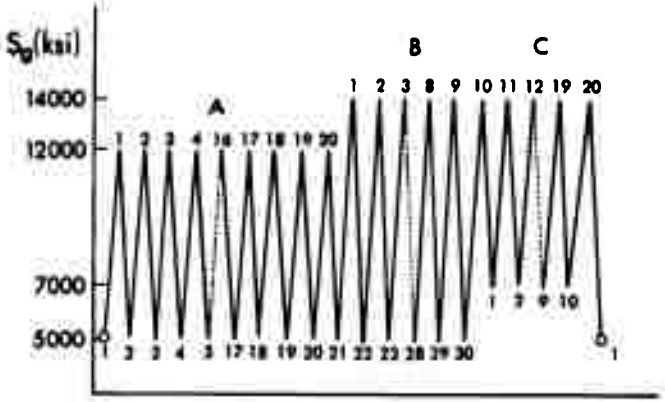


Figure 4c Program P13.

Programs P5 and P10 will be called random programs, although we know they are not truly random. Program P13 was designed to separate the influence of a change of maximum load and of a change of load amplitude on the rate of crack propagation.

## III. RESULTS

### Fatigue Cracking and Striation Formation

In order to understand clearly the relationship between striation spacing and load cycles, the mechanism of striation formation should be explained.

All the fatigue striations observed in this work were of the ductile type.[12] The fatigue striations, which are well resolved at high magnification, show a ridge or "sawtooth" profile with light and dark sides on each side of the ridge. The replicas were the two-stage plastic-carbon type shadowed in the direction of crack propagation. By comparing the contrast resulting from shadowing, we can determine unambiguously the slope orientation on each side of a striation. In one case, shadowing was done in a direction opposite to the direction of crack propagation to reverse the contrast and verify our conclusions. Matching areas on opposite faces of the fracture surfaces were also studied and some stereo micrographs from one side of the fracture surface were examined. All these different techniques led to the following conclusions, which are summarized in the sketches of Figures 5 and 6:

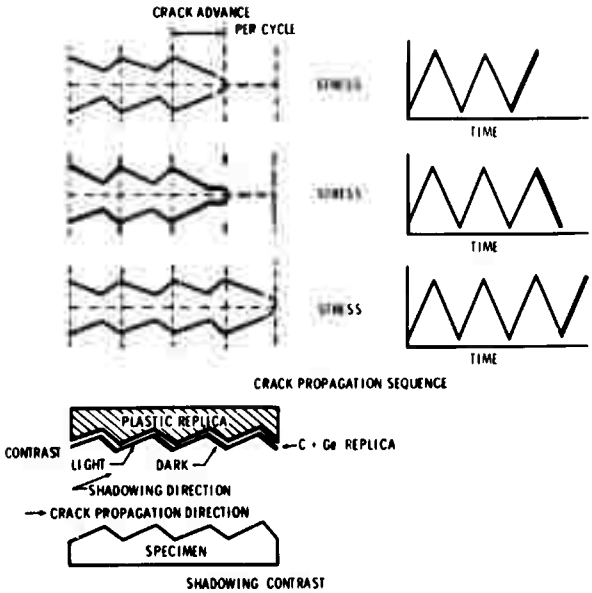


Figure 5 Sketches showing the formation of a striation. Crack advance occurs only during the load rise part of the load cycle.

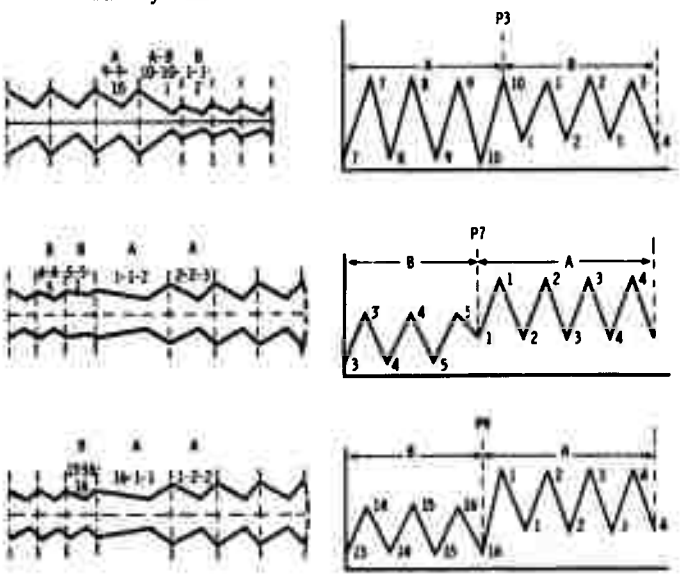


Figure 6 Sketches a, b, c show the striation profile and spacing for parts of Programs P3, P7, and P9.

1. The dark side of the striation (on either of the fracture halves) always faces the crack front when shadowing is in the direction of crack propagation. By opposition, the brighter part of the fatigue striation faces away from the crack front. The dark side of the striation always has a rumpled appearance with fine, wavy, "slip" lines which are usually parallel to the crack front, indicating heavy deformation. The bright side of a striation is flat and generally featureless. The relative width of the dark to bright sides of a striation is quite uniform for a constant cyclic load. Changes of maximum load or load amplitude result in marked changes in striation spacing, striation contrast, and relative widths of the bright to dark sides of a striation.

2. Fatigue cracking occurs only during a load rise, or opening of the crack, and it accounts for the entire crack extension. Figures 7 and 8, showing striations developed during Programs P11 and P12, demonstrate this finding clearly. In Figure 7 the large bright striation is due to the load rise B21-A1 at the beginning of Spectrum A, and in Figure 8 it is due to the load rise A4-B1 at the end of Spectrum A.

3. During unloading, or closing of the crack, the two fracture surfaces created during the preceding stress rise are heavily deformed near the crack tip. This leads to the formation of the dark, rumpled side of the striation and erases, in part, the bright appearance of the fracture face created during the loading part of the cycle. The ratio of dark to bright sides of the striation depends


Figure 7 Typical fracture surface resulting from Program P11. Note the large striation spacing due to the load amplitude B21-A1 (9000 psi) followed by three large striations corresponding to the load cycles of Spectrum A (2a = 1.7 inches).

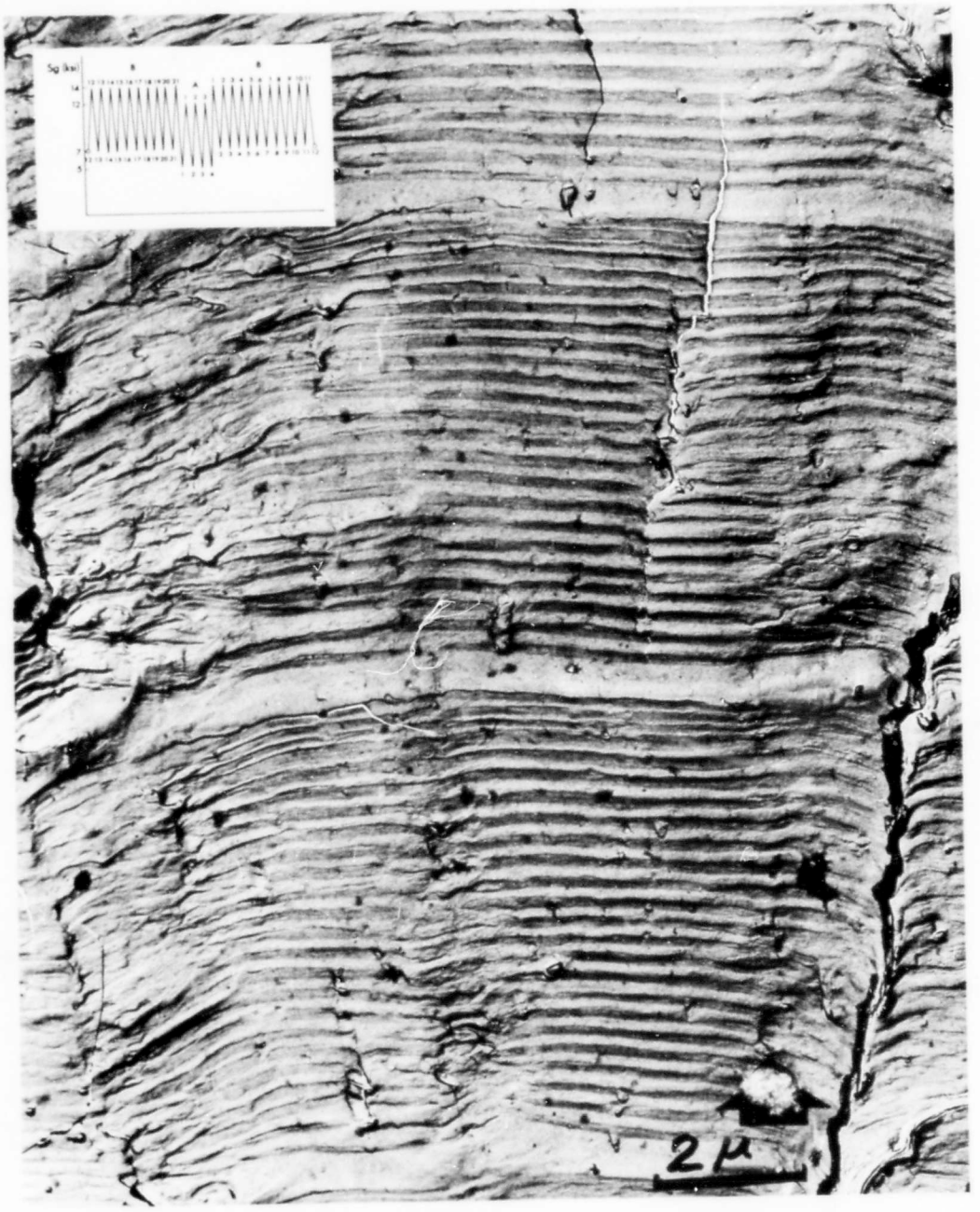


Figure 8 Typical fracture surface resulting from Program P12. Note the large striation spacing due to the load amplitude A4-B1 (9000 psi) preceded by three smaller striations corresponding to the load cycles of Spectrum A (2a = 1.7 inches).

on loading *versus* unloading load amplitudes. But, even when the unloading load amplitude is much larger than the preceding load rise, the deformed width of the striation (dark side) is never greater than the crack advance due to the preceding load rise.

Figures 6a, 6b, and 6c illustrate different fatigue striation profiles and the corresponding load sequences. Since the exact shape and size of the crack tip is unknown, it is represented as a dotted line in each sketch. The height of the striations is magnified for better illustration.

Laird[13] has recently presented a review of fatigue cracking and striation formation. There is little doubt that, as was shown by Laird and Smith,[14] and by McEvily,[15] there is a sharpening of the crack tip during unloading. Resharpening of the crack tip takes place by heavy deformation on the shear planes at 45° to the plane of the crack at the crack tip. This deformation, which can be called a macrocooperative slip or shear, can take place in noncrystalline as well as in crystalline materials. In the case of crystalline materials the orientation of a grain and the slip systems available may facilitate the resharpening process by a dislocation mechanism similar to the one suggested by Schijve.[16] Most of Laird's[14] observations were made on fracture surfaces resulting from low cycle fatigue. That is, there was always enough deformation or shear at the crack tip to create a well-defined groove, regardless of the crystallography of the materials. On the other hand, in the case of high

cycle fatigue -- that is, growth rates smaller than one micron/cycle -- the fine fatigue striations are not observed in all the alloy systems. Striations are well defined for the 2024 alloys, they are sharp and angular in the 7000 series aluminum alloys, very irregular in titanium alloys, and rarely defined at all in high strength steels. In conclusion it can be stated that:

1. Striation formation is a two-step process, with crack extension on the loading portion of the stress cycle followed by striation definition through plastic flow and resharpening of the crack on the unloading portion of the stress cycle, and,
2. The crystallography of the material can accentuate the localization of this flow leading to sharp, well-defined ridges and grooves.

At this point, before presenting the results, it is worthwhile to stress the fact that crack propagation by striation formation is the principal mechanism of fatigue crack propagation for short crack lengths and slow growth rates; that is, for our tests, for $0.500" < 2a < 1.5$ to 2 inches. Figure 9 shows typically the uniformity of crack propagation by striation formation. Striations are formed right at the root of the notch as soon as the crack starts propagating, as shown in Figure 10. Stage I[12] crack growth was not observed.


Figure 9 Note the uniformity of the striation spacing and the extent of fracture surface covered by striations. Program P11 (2a ≈ .6 inch).

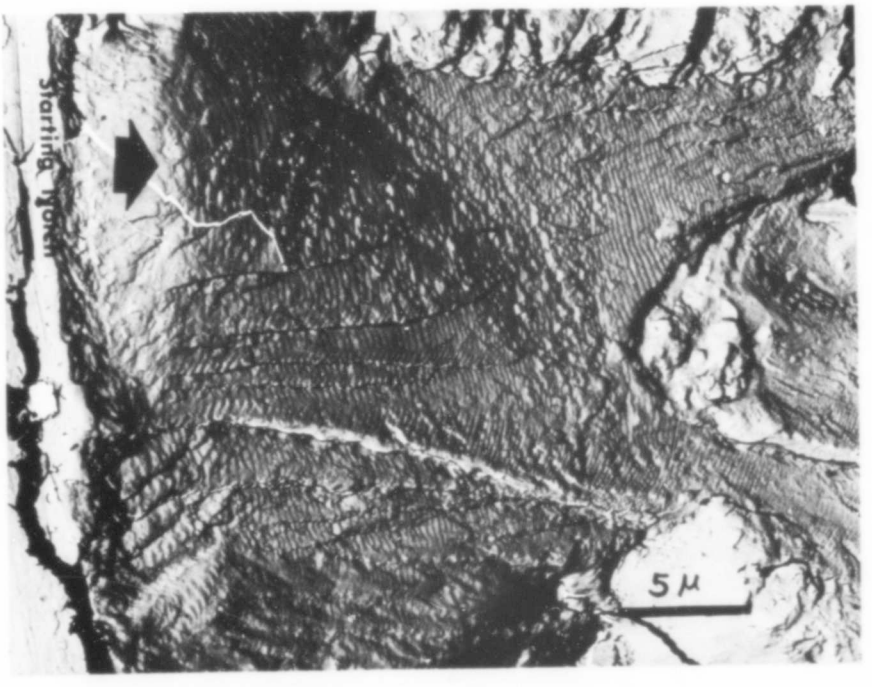


Figure 10 Crack propagation by striation formation (Stage II) starts right at the root of the sawtooth notch. Program P11 (2a = .5 inch).

Constant Maximum Load and Variable Load Amplitude Programs

Five programs, P1 to P5, with constant S max and variable ΔS were planned and tested. The test data are reported in Figures 11 and 12, which represent plots of crack length *versus* crack growth rates.

Programs P1 and P2 were designed and run first. There was no significant difference in crack growth rates between the two programs. The fracture surfaces did not show any striations or crack growth for Spectrum A (ΔS = 2000 psi) of either program. Consequently the programs could not be differentiated by examination of the micrographs alone, since the absence of striations due to Spectra A resulted in the same spectra sequence for the two programs; that is, BCBCBC for P1 and CBCBCB for P2. Figures 13, 14, and 15 show typical fractographs for Programs P1 and P2, respectively. The only significant feature besides the change in striation spacing between Spectrum B and Spectrum C was a brighter striation corresponding to C77-A-A9B1 in P1 and to C77-B71 in P2. In P2 this striation had the same spacing as the other striations in Spectrum C, but appeared brighter because of the smaller width of the dark part of the striation, which corresponded to the smaller unloading amplitude C7-B1. In P1 the bright striation had the same appearance as in P2 but appeared to be larger than the other C striations, which would mean that Spectrum A resulted in some limited crack extension but with no resolvable striation formation. Spectrum A does not

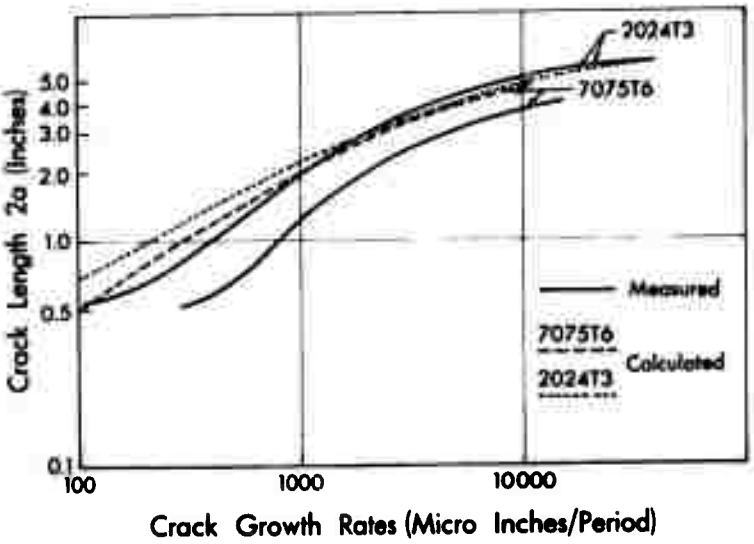


Figure 11 Crack length *versus* crack growth rates for Programs P1 and P2, and alloys 2024-T3 and 7075-T6.

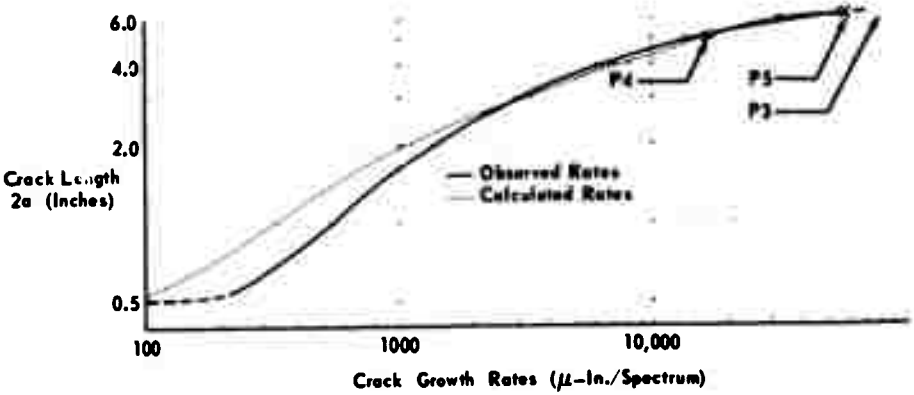


Figure 12 Crack length *versus* crack growth rates for Programs P3, P4, and P5.

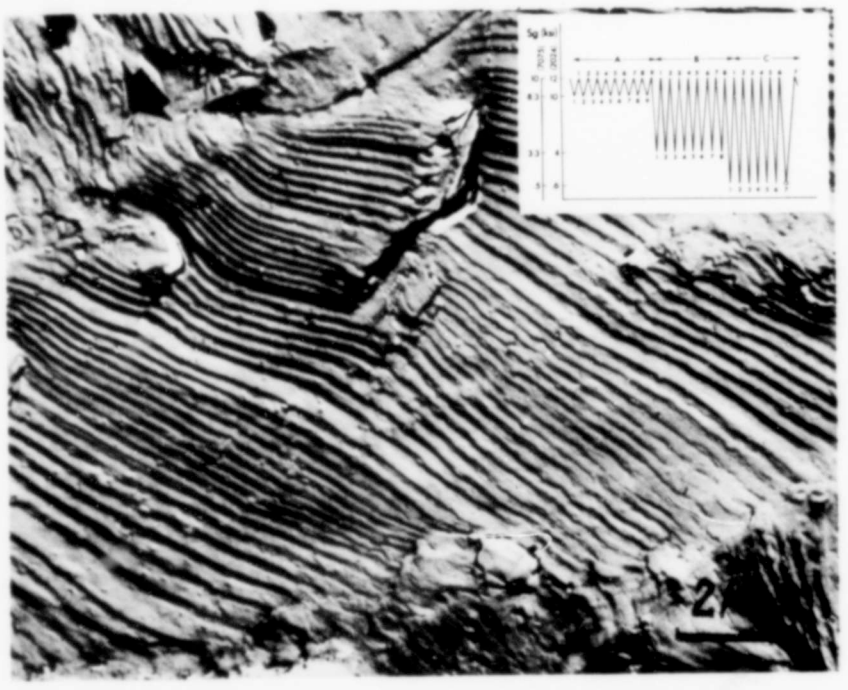

Figure 13 Typical fracture surface due to Program P1. (2a = .7 inch)

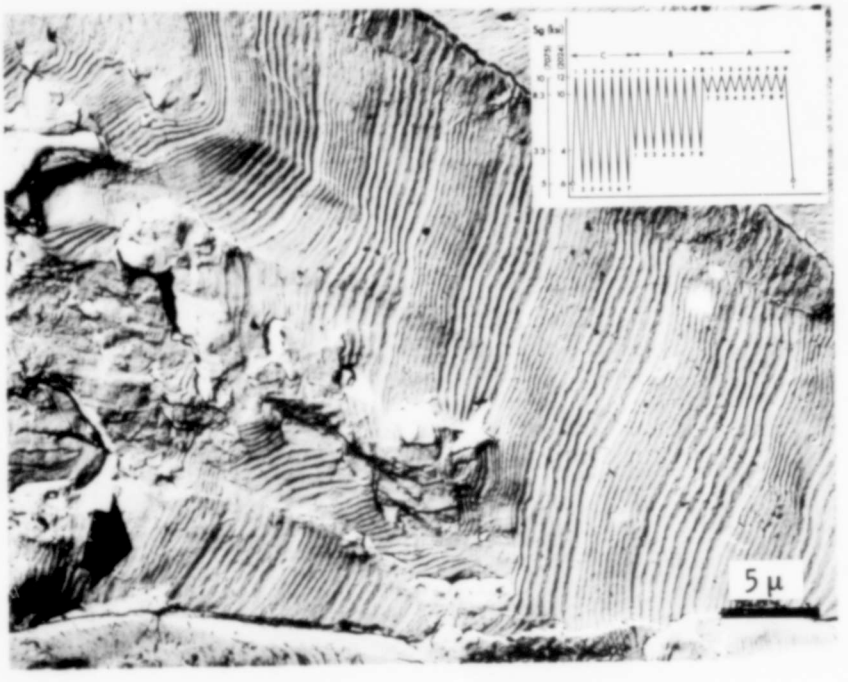


Figure 14 Typical fracture surface due to Program P2. Compare with Figure 13. (2a = 1.3 inches)

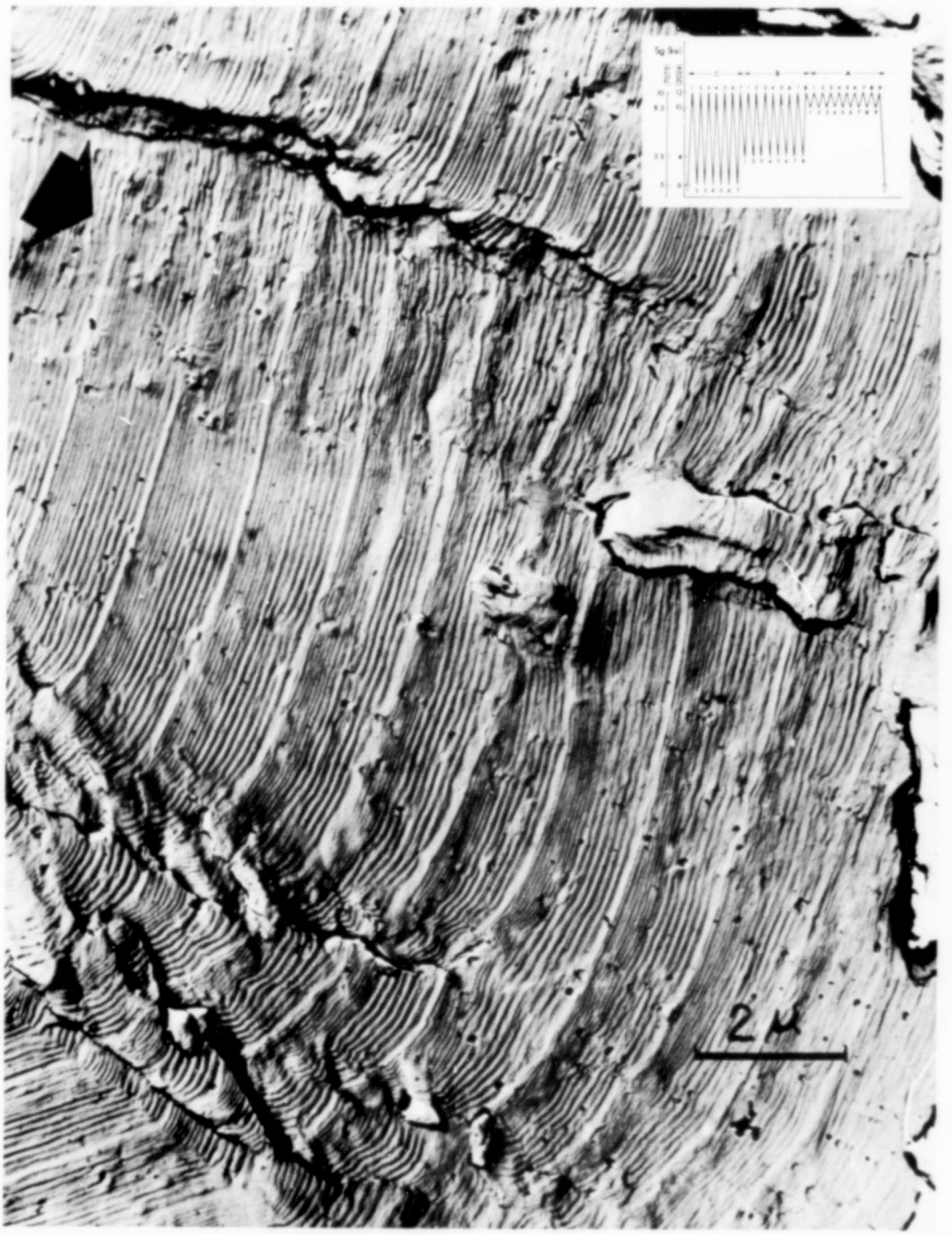


Figure 15 Typical fracture surface due to Program P2, showing the uniformity of striation spacing (2a = .6 inch).

show up even at the longest crack lengths whereas striations are still observed for Spectra B and C amidst large regions of ductile tear.

Program P3 was designed as a modified P2, with $\Delta S$ = 6000 psi for Spectrum A and a different number of cycles in each spectrum. This time Spectrum A resulted in well-defined A striations between striations C and B, as shown in Figures 16 and 17. Programs P4 and P5 were then designed and run. Characteristic fractographs are shown in Figures 18 and 19.

Figure 12 gives a log-log plot of observed and calculated crack length *versus* growth rate per program for P3, P4, and P5 (for P4 the rates plotted correspond to a half program). The crack growth rates for the random case, P5, were the same as for the programmed spectra, P3 and P4. This shows that in the tests at constant maximum load the sequence of load application did not measurably influence the overall crack growth rates. This was confirmed by the fracture analysis with the electron microscope:

1. There was no marked crack front advance at the change of load amplitude between different spectra.

2. After a change of load amplitude, the spacing of the striations for the next load amplitude sequence reached a stable and uniform value on the first cycle of the new load amplitude sequence.

The average rates of crack propagation per load cycle for each load amplitude sequence in Programs P3 and P4 were measured for

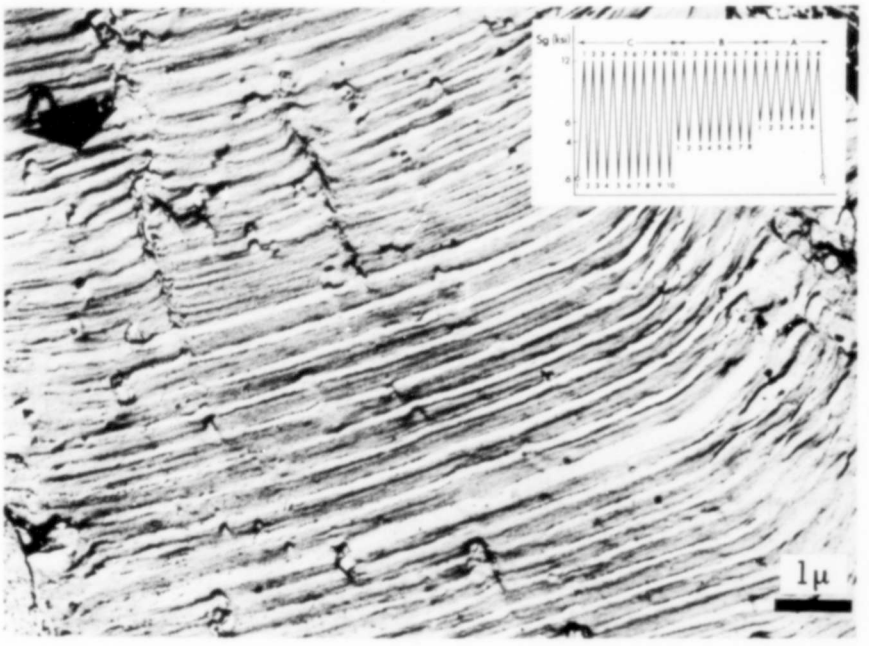


Figure 16 Typical striation profile corresponding to Program P3 (2a = 0.9 inch).


Figure 17 Typical fracture surface, showing the uniformity of the striation spacing for the three spectra of Program P3 (2a = .7 inch).

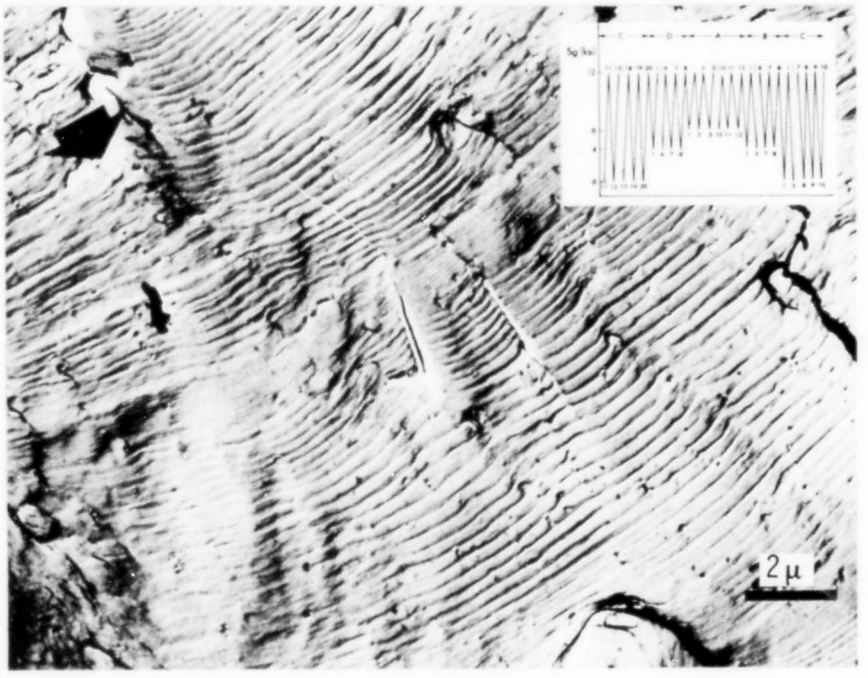


Figure 18 Typical fracture surface due to Program P4. The sequence of application of the load amplitudes does not seem to change the striation spacing markedly (2a = .9 inch).

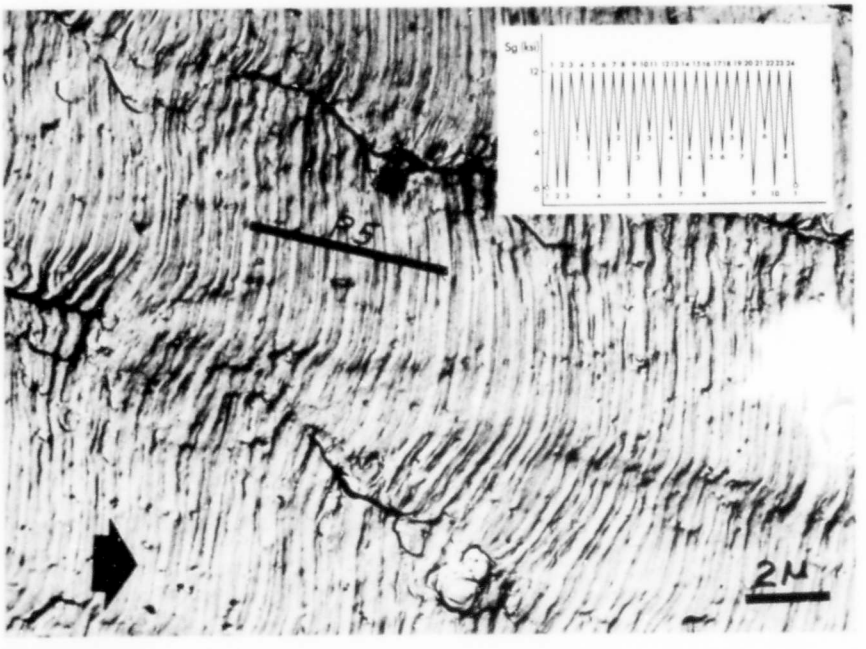


Figure 19 Striation profile corresponding to pseudorandom Program P5 (2a = .9 inch).

various crack lengths between $2a = 0.5$ inch and $2a = 0.9$ inch. The growth rates per cycle in each field of view were compared with the larger growth rate (taken as unity) corresponding to $\Delta S = 11{,}400$ psi. This procedure partially eliminated the scatter in absolute growth rates, which is always observed at high magnification even at a constant crack length.

Figure 20 is a plot of log $\Delta S$ *versus* log relative crack growth rate per cycle. There was a certain scatter in the data, but it showed that, for constant S max, the following relative crack rate equation could be written:

$$\text{rate} = C(\Delta S)^n \tag{1}$$

with $n = 1$ for $\Delta S$ between 8000 and 12,000 psi, and increasing from two to four for $\Delta S$ lower than 8000. It is unfortunate that we were not able to extrapolate this plot for $\Delta S = 2000$ psi. The possibility that measurable growth could be achieved by large increases in the numbers of stress cycles at $\Delta S = 2000$ psi was considered, but no testing to investigate this point was conducted.

Constant Load Amplitude and Variable Maximum Load Programs

Seven programs, P6 to P12, with constant $\Delta S$ and variable S max were planned and tested. The test data are reported in Figures 21, 22, and 23, which represent plots of crack length *versus* crack growth rates.

There was no significant difference in macroscopic crack

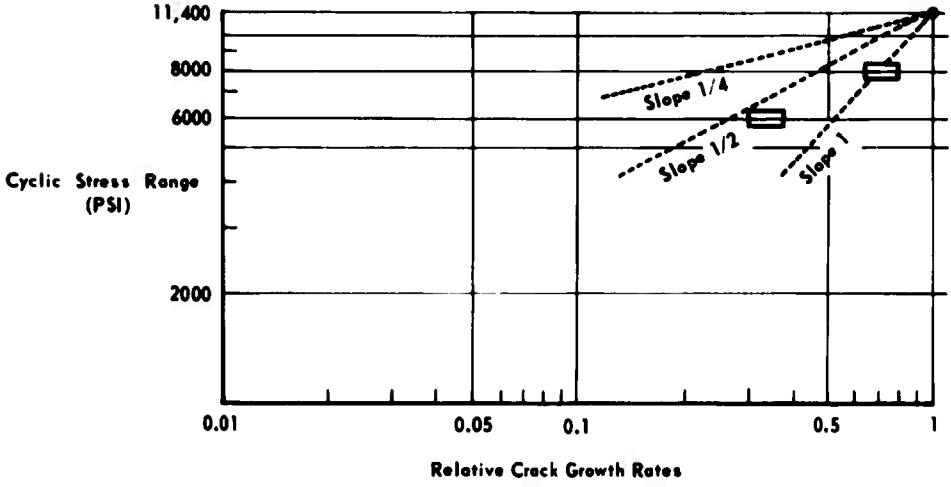


Figure 20 Relative crack growth rates at constant S max for Programs P1, P2, P3, and P4.

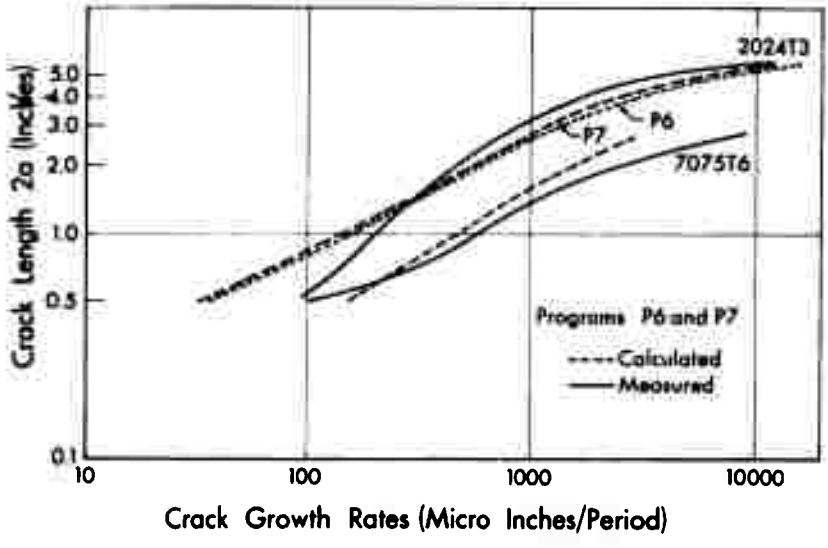


Figure 21 Crack growth rates *versus* crack length for Programs P6 and P7.

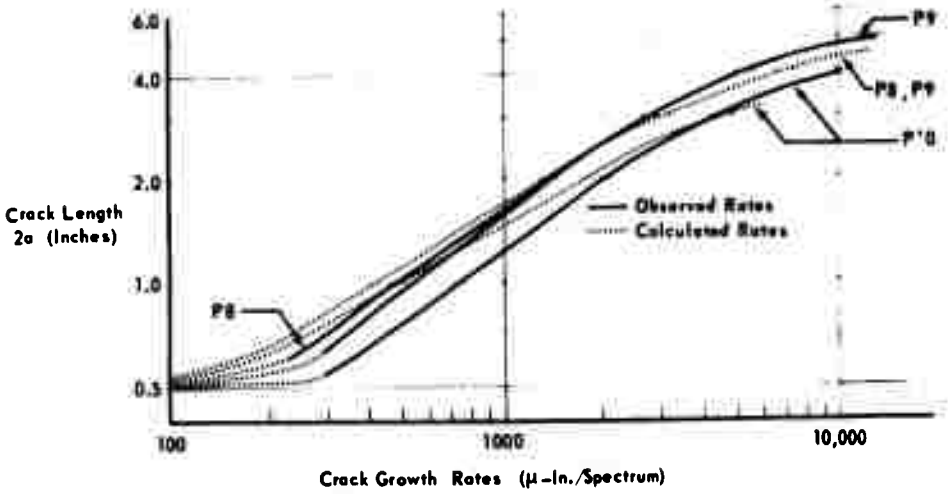


Figure 22 Crack growth rates *versus* crack length for Programs P8, P9, and P10.

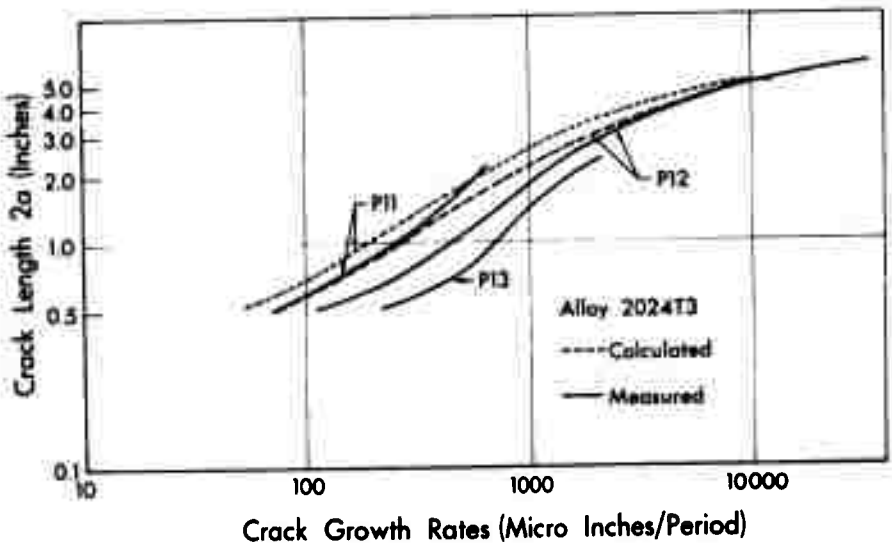


Figure 23 Crack growth rates *versus* crack length for Programs P11, P12, and P13.

growth rates between Programs P6 and P7. The striations observed on the fracture surface were never as well defined as for Programs P1 to P5. However, Spectra A, B, and C of P6 could be easily identified, as shown in Figure 24. Spectrum D did not show any crack advance or striations but accounted for a very narrow and sharp compression groove before the large crack jump at D7-A1, which corresponds to the largest change in load amplitude for P6. The crack jump due to this load change was equivalent to the total crack advance due to the three following cycles, A12, A23, and A34.

Program P7 was similar to P6. That is, Spectra C, B, and A were easily identified on the fractographs, and Spectrum D did not result in any visible cracking. Each change of maximum load at C66-61-A11 and B55-51-A11 created a larger striation spacing, as shown in Figure 25. The crack jumps and the corresponding striation profiles between Spectra B and A are sketched in Figure 6. The sketch shows clearly the marked difference in striation spacing between cycle A11-12 and the following cycles A22-23, A33-34, and A44-A4D1, although all these cycles had the same load amplitude and the same maximum load.

Programs P6 and P7 proved difficult to analyze, with too many load levels and too few cycles at each load level. For this reason, Programs P8, P9, and P10 were designed and tested. Figure 22 presents a plot of log crack length *versus* log macroscopic crack growth rates for P8, P9, and P10. At lower growth rates P9 was faster than

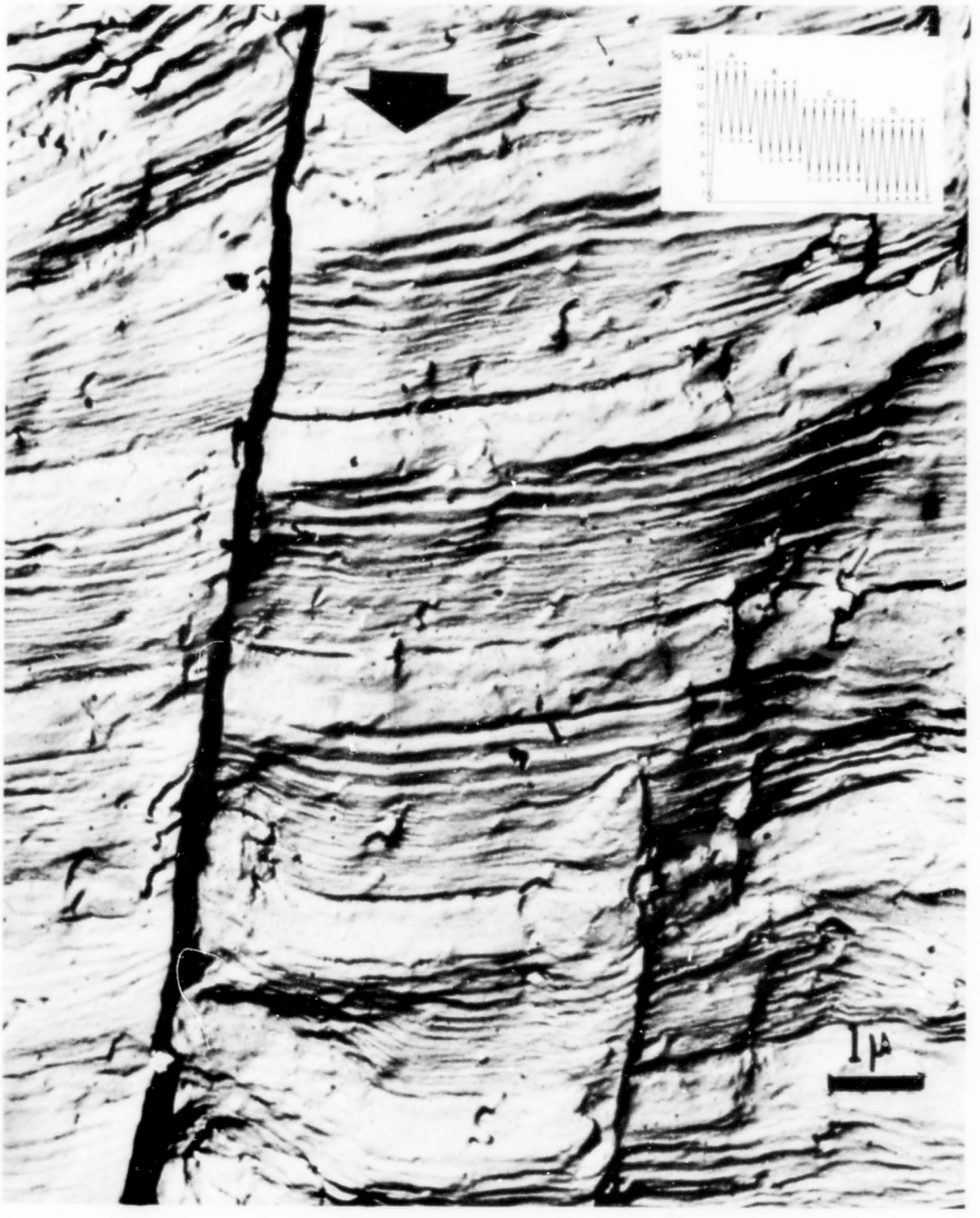

Figure 24 Typical fracture surface due to Program P6. Note the large crack jump corresponding to D7-A1 (2a = .9 inch).

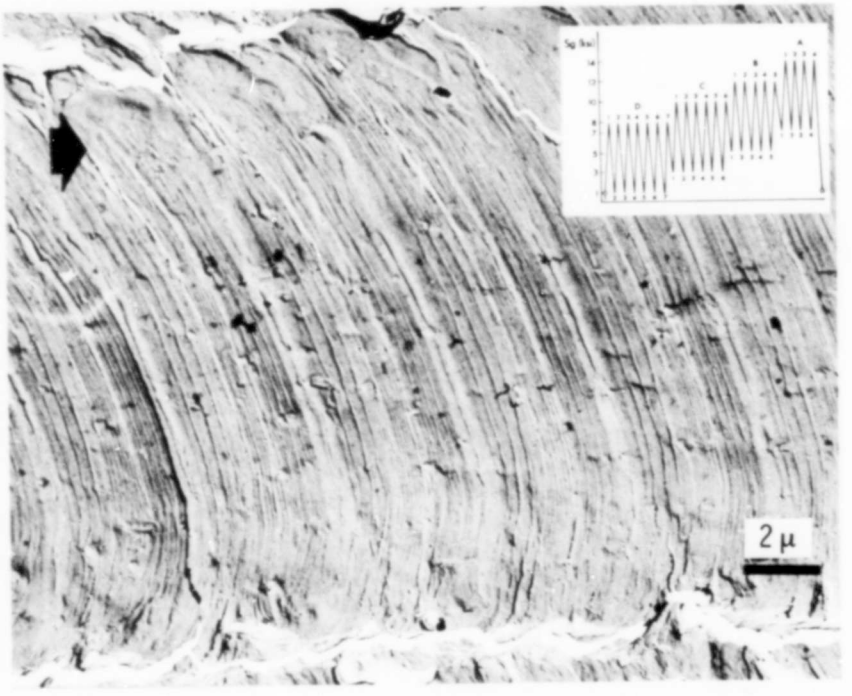


Figure 25 Typical fracture surface due to Program P7 (2a = 1.7 inches).

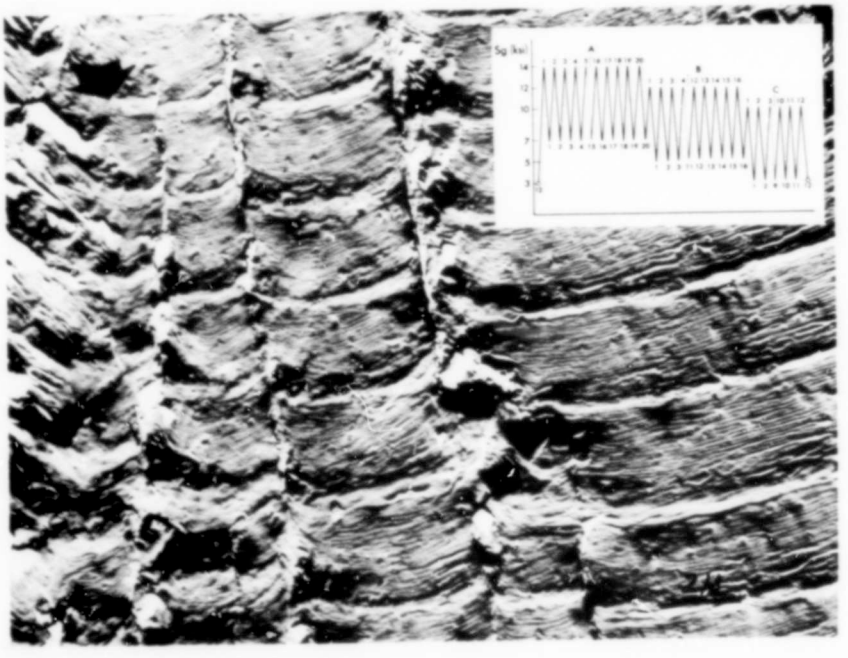

Figure 26 Fracture surface topography due to Program P8.

P8, while the random program P10 was always faster than P8 or P9. Figures 26, 27, 28, and 29 show typical fractographs of P8, P9, and P10. Spectra A and B are well resolved, with all the striations accounted for. The cracking due to Spectrum C cannot be resolved on the micrographs. The crack jumps due to change in maximum load levels P9-A20-C1 and P9-C12-B1, and P9-B16-A1 are clearly identified.

The average microscopic rates of crack growth per load cycle for Spectra A and B of Programs P6, P7, P8, and P9 were measured within each program and compared with the larger growth rate (taken as unity) corresponding to S max = 14,000 psi. The effect of the maximum load amplitude on the relative crack growth rate per cycle is shown in Figure 30. The scatter was quite large, but a relationship of the type:

$$\text{rate} = \text{constant}(S\ \text{max})^{m} \qquad (2)$$

could be written to represent relative crack growth rate. At a given crack length and for a constant maximum load, m varied from two to three at large S max to three to five at smaller S max. In the same figure the relative microscopic rates confirm the fact that P9 had a larger growth rate than P8. This can be explained by assuming a crack growth retardation in Spectrum B of P8 because Spectrum B followed the higher load level of Spectrum A. The crack growth retardation could be due to a work softening of the plastic zone by Spectrum B and a consequent lower crack growth rate.

Program P10, as expected, was much faster than P8 and P9.[11]

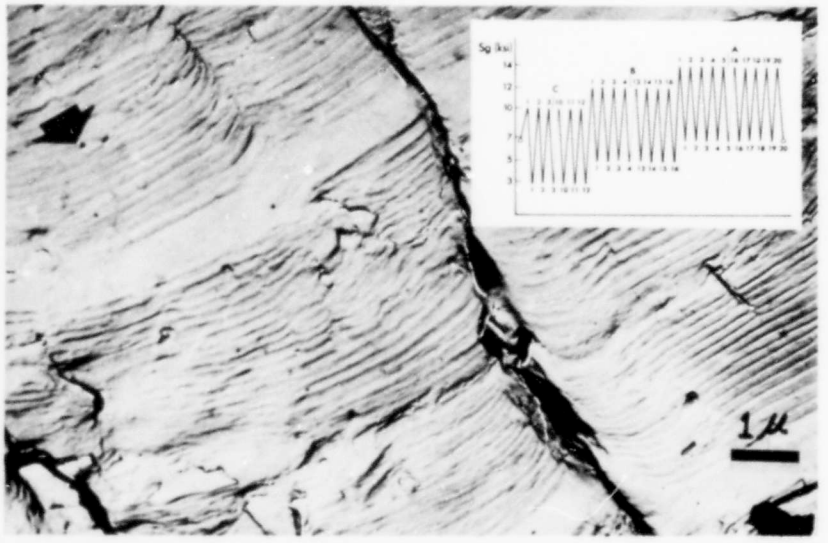


Figure 27 Fracture surface topography due to Program P9 (2a = .9 inch).

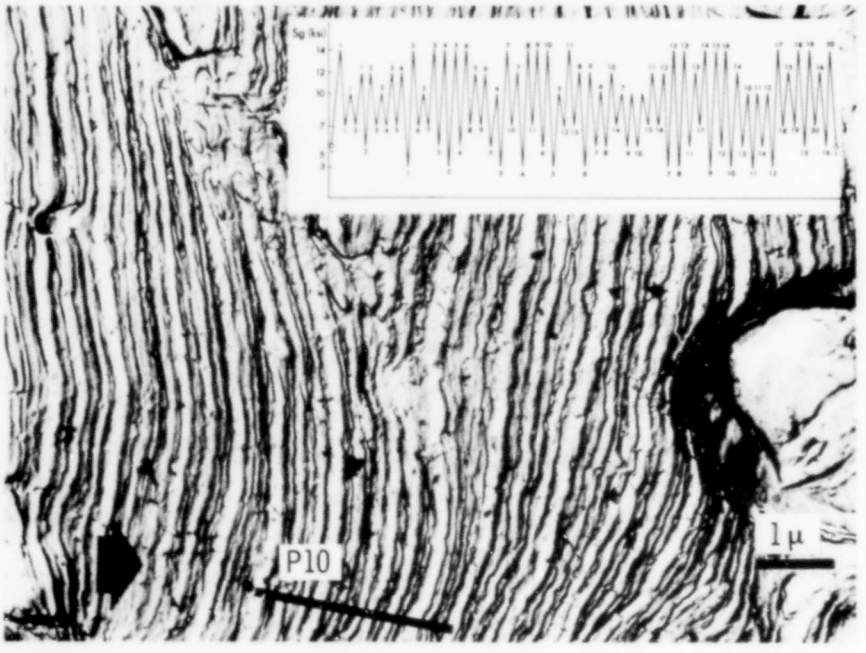


Figure 28 Fracture surface topography due to Program P10 (2a = .6 inch).


Figure 29 Fracture surface topography due to Program P10. Note the sharpness of the striation ridges, indicating a sharp crack tip (2a = .6 inch).

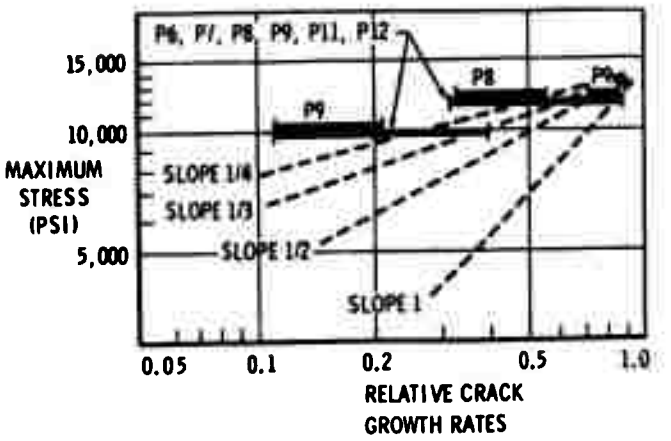


Figure 30 Relative crack growth rates at constant load amplitude, variable maximum loads, for Programs P6, P7, P8, and P9.

The large number of high load rise amplitudes coupled with many changes of load level accounts for this large difference in growth rates. In Figures 28 and 29 the striation spacings and profiles can be related to the applied random loads if S max, $\Delta S$ , and prior S max are considered. With few exceptions, only striations due to S max = 14,000 psi are clearly resolved. This implies that S max effects are more important than $\Delta S$ or prior S max effects.

Programs P11 and P12 were designed to show that cracking takes place only during the opening of the crack. The test data are reported in Figure 23, which shows plots of crack length *versus* crack growth rates. Spectrum A in P11 did not result in any crack arrest since all the cycles of Spectrum B could be counted; on the contrary, the first striations of Spectrum B were often observed to have a slightly larger spacing than the last one. This crack acceleration at a lower level following a high load level was not clearly observed in P9.

Program P13 complements P11 and P12. In P11 and P12 a change of maximum load level is always accompanied by a change of load amplitude and it is impossible to separate the effect of load level and load amplitude. This can be done in P13 by comparing the striation spacing due to cycles A21-B1 with the following cycles, B22-2, B33-3, etc. It can be seen in Figures 31 and 32 that the first cycle at the higher load level creates a larger crack advance than the following cycles. As will be discussed later, this can be explained by con-

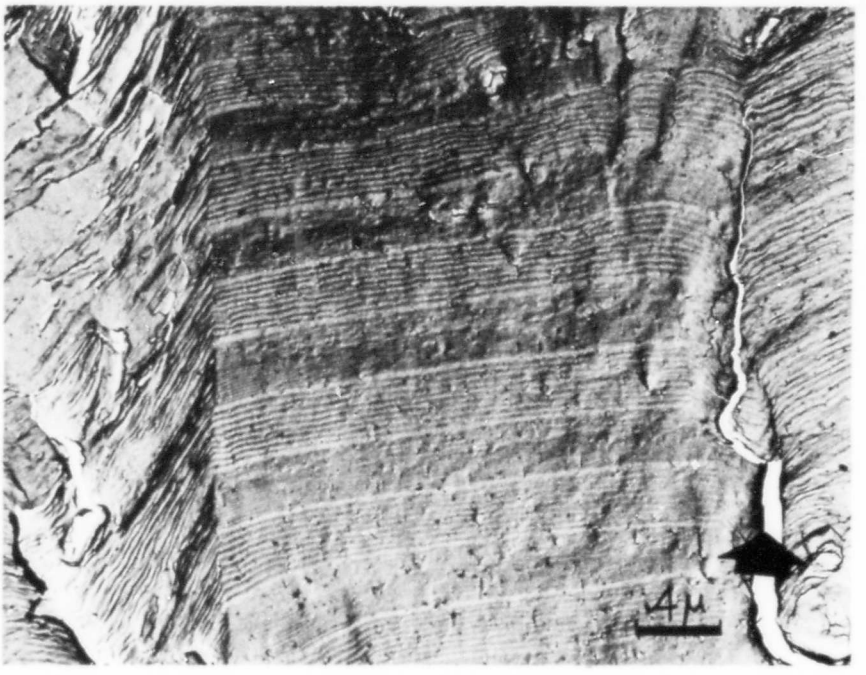


Figure 31 Fracture surface topography due to Program P13 (2a = .9 inch).

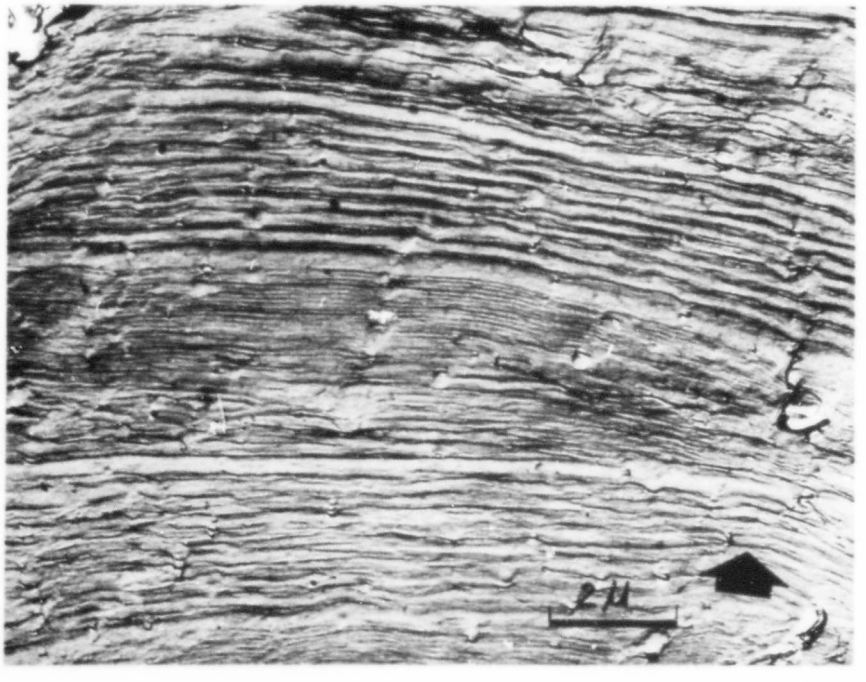


Figure 32 Fracture surface topography due to Program P13. Note the large striation spacing corresponding to A21-B1 (2a = .9 inch).

sidering the difference in notch effect due to different crack tip shapes and radii prior to a change in load level.

Computed Crack Growth Rates

An available computer program was used to calculate the crack growth rates of all the programs tested. The crack growth data used in the computer program were taken from previous tests at constant S max and constant ΔS values. These "in house" data correspond to different heats of material, and the difference between computed and measured growth rates can be attributed to chemistry, environment, and testing variables. However, since one practical aim of fatigue cracking tests is to predict random and programmed crack growth from load-crack growth data, an attempt was made to use these data for our programs. The computer calculated the crack advance for each load cycle and consequently took into account the large changes in load amplitude at each change of maximum load level. The computed data showing crack length *versus* number of periods are given in Appendix II. Figures 11, 12, 21, 22, and 23, giving crack length *versus* crack growth rates also show the computed curves of crack length *versus* growth rates.

All the computed growth rates were slower than the observed macroscopic rates for the same crack length between $2a = 0.5$ inch and $2a = 2$ inches. At larger crack lengths the computed rates were equal to the observed rates, and, in many cases, at very large crack lengths the computed rates were faster than the observed rates. We

see that the computed growth rates differ from the measured rates by a factor less than two, but the calculated rates are not conservative in the long life region. This conclusion is better illustrated in Table IV, which compares the measured and calculated number of periods to achieve the same crack growth (from .5 inch to near critical crack length). The column giving $\sum \frac{n}{N}$ shows the deviation from Miner's rule.

## IV. DISCUSSION

The different program load sequences have clearly demonstrated that crack extension in 2024-T3 aluminum alloy occurs only during the stress rise part of a load cycle, but the striation profile and appearance depend on both the loading and unloading amplitudes of the load cycle. The smallest striation spacing observed was of the order of one μinch or 250 Å. The resolving power of the replicating technique is approximately 100 Å. In all the programmed load tests, whenever the striations were defined well enough to be easily counted, we found a perfect one-to-one correlation between the number of striations and the number of load cycles in a spectrum. In the random programs, P5 and P10, correlating striation spacing to load cycles in the program was more difficult, but with some time and effort it was done for all the micrographs taken. With training one can, by looking at a random load spectra, select the load levels and load amplitudes which will account for the largest striation spacings observed on the fracture surface. In

TABLE IV

CALCULATION OF $\sum \frac{n}{N}$ FOR CRACK PROPAGATION

(2a = .5 inch)

| Programs | 2a* | N Calculated | n Measured | $\sum \frac{n}{N}$ |
|---|---|---|---|---|
| Alloy 2024-T3 | | | | |
| P1 | 6.00 | 7956 | 4950 | .625 |
| P2 | 6.00 | 7956 | 5340 | .675 |
| P3 | 6.50 | 5526 | 3639 | .658 |
| P4 | 5.40 | 5526 | 3639 | .658 |
| P5 | 6.50 | 5526 | 3610 | .650 |
| P6 | 5.80 | 12151 | 10755 | .885 |
| P7 | 4.59 | 13320 | 11900 | .900 |
| P8 | 5.80 | 4440 | 3855 | .870 |
| P9 | 5.30 | 4450 | 3675 | .830 |
| P10 | 2.80 | 3500 | 2275 | .650 |
| P11 | 2.90 | 8970 | 7900 | .885 |
| P12 | 5.80 | 6942 | 5060 | .730 |
| P13 | - - - - - - - - - Not Calculated - - - - - - - - - | | | |
| Alloy 7075-T6 | | | | |
| P1 | 4.08 | 5500 | 2700 | .490 |
| P2 | 3.69 | 5410 | 3981 | .730 |
| P6 | 2.70 | 3468 | 3275 | .945 |
| P7 | 2.26 | 3460 | 2450 | .710 |

* 2a represents the maximum crack length calculated by the computer program.

summary, this work was very valuable in gaining an understanding of the mechanisms of formation and the appearance of fatigue striations. This understanding is being directly applied to the evaluation of crack propagation in test components and service parts subjected to simulated or real load programs.

The microscopic crack growth rate measurements for Programs P1 to P5 and P6 to P12 yield the following empirical equation of crack growth rate by combining Equations (1) and (2):

$$\text{growth rate} = \text{constant } (\Delta S)^n (S \text{ max})^m \qquad (3)$$

Like the measurements from which it is derived, this empirical equation gives a relative change of growth rate at a given crack length for relative changes of $\Delta S$ and S max. Equation (3) applies to a stabilized growth rate with uniform striation spacings at a given $\Delta S$ and S max load level. It does not apply exactly to the growth rate corresponding to the one large striation created by the first load cycle of a higher load level. The exponent $n$ varies from one to three and up to four for decreasing values of $\Delta S$. For $\Delta S$ ranging from 8000 psi to 11,400 psi it is surprising to find $n = 1$, since Paris[18] has shown that $n = 4$ is a general trend in fatigue crack growth. The only explanation for this difference can be given in terms of S max. Most of the tests with variable $\Delta S$ were conducted (see Schijve) at constant S mean, which means that S max varies at the same time as $\Delta S$; consequently the changes of growth rates are the result of combined changes of $\Delta S$ and S max. As it will be shown

later, changes of S max can markedly influence the growth rates. It would be interesting to do more testing to measure accurately the dependence of growth rates on $\Delta S$ at constant S max. For $\Delta S$ varying from 8000 psi to 6000 psi and 2000 psi n increases to two or three. This increase corresponds to smaller growth rates than expected at low $\Delta S$ as a result of crack retardation, or even arrest, following the application of loads with a large $\Delta S$. The most striking result at constant S max is the independence of the crack growth rate with respect to the sequence of load amplitude application.

In Equation (3) the exponent m, which relates S max to the growth rate, varies from three to four and up to five when S max varies from 14,000 psi to 10,000 psi. Schijve had found $m \approx 3$. This large dependence of the crack growth rate on the maximum stress level accounts for the marked change in striation spacing whenever the maximum load level is changed. It also explains the fact that in a random load test the peak loads result in large crack jump with large, well-defined striations.

Table IV shows that the prediction of crack growth rates, using Miner's rule, was unconservative for all the test programs run. It is interesting to note that the prediction was better for the Programs P6 to P12 with variable maximum loads, than for Programs P1 to P5 with constant maximum loads. This can be easily explained if, for Programs P6 to P12 the higher load levels have a marked de-

celerating effect on crack propagation at the lower load levels.

In Table IV it is also interesting to note that $\sum \frac{n}{N}$ for the pseudorandom Program P10 is much smaller than for the other Programs P8 and P9, which shows that estimation of random load crack growth rates is less accurate than estimation of programmed load growth rates.

It is clear by now that the application of Miner's rule to predict crack growth rates does not give a satisfactory answer. For the tests reported here we found $\sum \frac{n}{N}$ varying from .65 to .85 (unconservative prediction), while Schijve[11] found values of $\sum \frac{n}{N} = 3$ for programmed load tests with peak overloads. In order to be able to predict crack growth rates for random and program loads we have to be able to account quantitatively for the three following observations:

1. Crack acceleration or crack deceleration,
2. Crack arrest,
3. Crack jump at a change of load level.

Crack Acceleration or Crack Deceleration

It is well known[11] that high stress amplitudes have a decelerating effect on the subsequent crack propagation rates at a lower stress amplitude and *vice versa* for the reverse sequence of low-high loads. Hardrath[21] shows (using his symbolic writing) that values of $\sum \frac{n}{N}$ for the following sequence $\triangleright\triangleright$ are equal to two or three times the value of $\sum \frac{n}{N}$ for the sequence $\triangleleft\triangleleft$ . The overall

growth rates for Programs P6 and P7, P8 and P9 were not markedly different, although these programs are of the same type as the programs run by Hardrath. The difference between Hardrath's tests and ours is probably due to the limited number of cycles at each load level in our programs. The difference in growth rate at the lower load levels is not as striking as would be expected for a large number of cycles.

The accelerating and decelerating effect is difficult to measure by electron fractography. It requires a comparison of absolute measurements of growth rates (striation spacing) at the same crack length or the same stress intensity factor between two difference fracture surfaces. The scatter in the measurements of striation spacing does not allow an accurate comparison. On the other hand, local changes of growth rates are easier to measure, and we have observed in the case of P11 that the first B cycles (17,000 psi) immediately following four A cycles (14,000 psi) result in a larger striation spacing than the last B cycles. Hertzberg[20] has made a similar observation for similar load programs. Therefore, in this case it seems that an abrupt decrease in load level is accompanied by a slow decrease in growth rates at the lower load level. The larger growth rates at the lower load level are certainly due to the fact that the material near the crack tip had been subjected to a deformation strain very close to the fracture strain, making cracking easy even at a lower load level.

Crack Arrest

After a high positive load, crack propagation at a lower

load level stops or is delayed for a certain number of cycles. (Schijve,[11] Plunkett[17]) In our programs crack arrest was observed for P1, P2, P6, P7, P8, and P9, and in each case only for the lowest load amplitude, or the lowest load level spectrum. It should be pointed out that crack arrest in some cases has been observed at the surface of a test specimen, but fractography shows that crack propagation is proceeding at the lower load level in the plane strain region, resulting in a "tunneling" of the crack front in the center of the test specimen. In general, however, crack arrest seems to take place over the whole crack front. Schijve[11] explains crack arrest on the basis of the building up and the elimination of residual stresses. This general explanation would need some experimental evidence to support it. For instance, the work of Hardrath[22] who measures the cyclic plastic stresses at a notch root, should be extended to see the rate of change of the residual stresses as a function of a change of load amplitude. It can also be said that we have paid little attention so far to the cyclic stress-strain hardening curve and how we can change the work-hardened state of a material from a monotonic workhardening to a cyclic workhardening. Following the application of a peak overload there is formation of a plastic zone at the tip of the crack which has been monotonically work-hardened. It is going to take a certain number of load cycles to reach the cyclic workhardening state typical of the plastic zone which controls fatigue cracking. When the plastic strain distribution within the plastic zone is found it will be possible to simulate the workhardening behavior of the plastic

zone with test bars subjected to controlled strain amplitudes increasing in the same way as the plastic strains at the tip of a fatigue crack.

Crack Jump at a Change of Load Level

A typical example is shown in Figure 33 where the first of six cycles at 28,450 psi corresponds to a large crack jump. Similar observations were made with Programs P6 to P13. It is felt that the crack tip radius and the related stress concentration factor will markedly influence the crack advance on the application of the first higher load cycle.

Although we partly understand the sequence of striation formation right at the crack tip, we still do not know the exact shape and size of the crack tip. It is difficult to see how we can get a better crack tip image with the existing tools and techniques. At this stage it is convenient to assume a uniform crack tip shape, with the crack tip radius $r$ becoming an important variable determining the intensity of the stress concentration at the tip of the crack. In a first approximation it seems that $r$ is closely related to the width of the part of the striation created during the closing mode of the crack, which is a measure of the resharpening of the crack tip during unloading. In the case of random load programs, resharpening of the crack tip to a very small $r$ value will be due to all the small load amplitude, low level load cycles. The peak overload will be more damaging in a random load sequence than in a program sequence because of the larger stress concentration at the

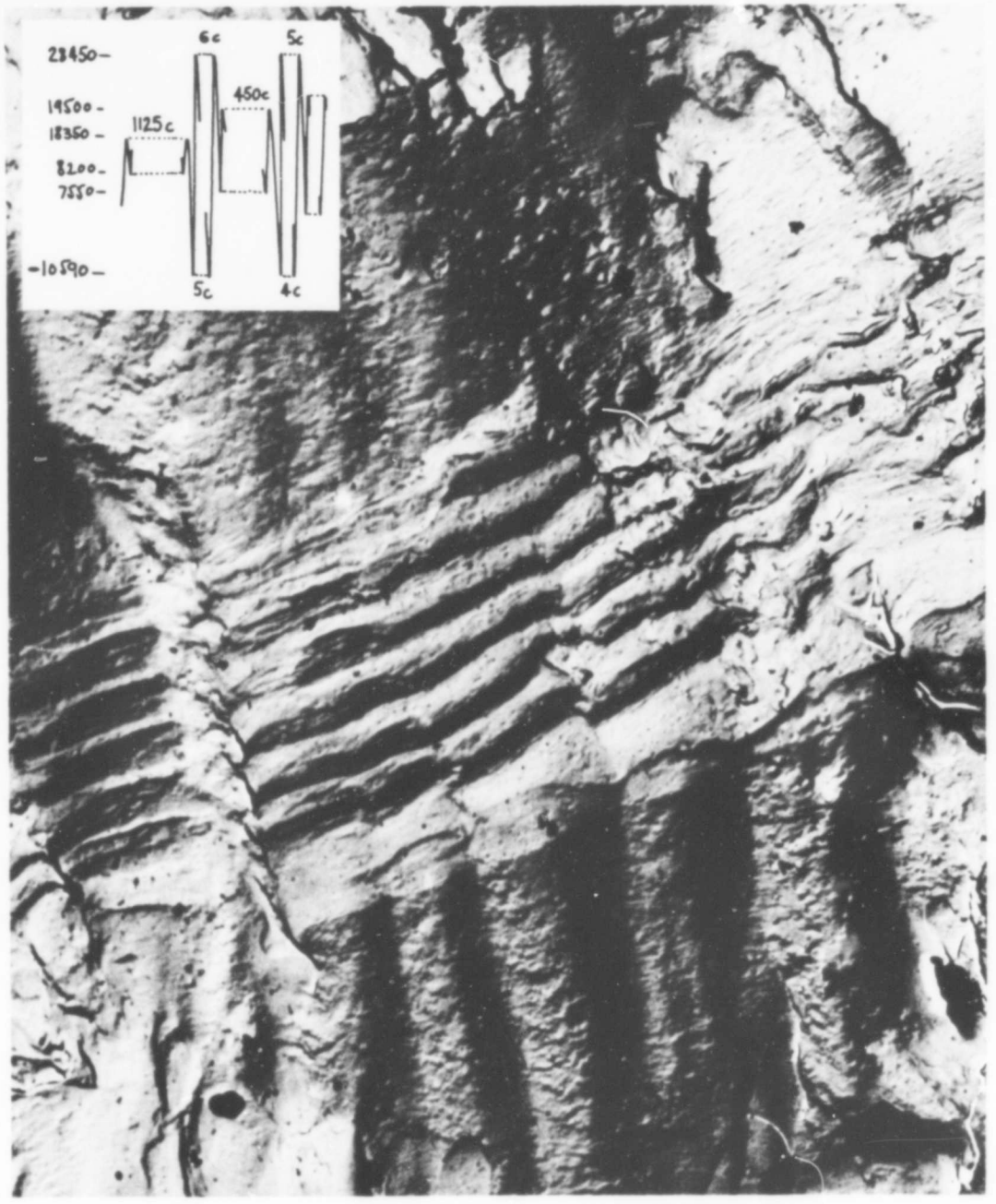


Figure 33a (courtesy of Rutkiewicz and Mavec, Wichita Division) Note the large crack jump occurring on the application of the first large load. The spacing of the first striation is larger than for the following five striations, although the load amplitude and level are the same. Use with Figure 33b to form a stereo image, and note the difference in crack tip profile after 1125 cycles at 18,350 psi and at each of the large load cycles (28,450 psi).

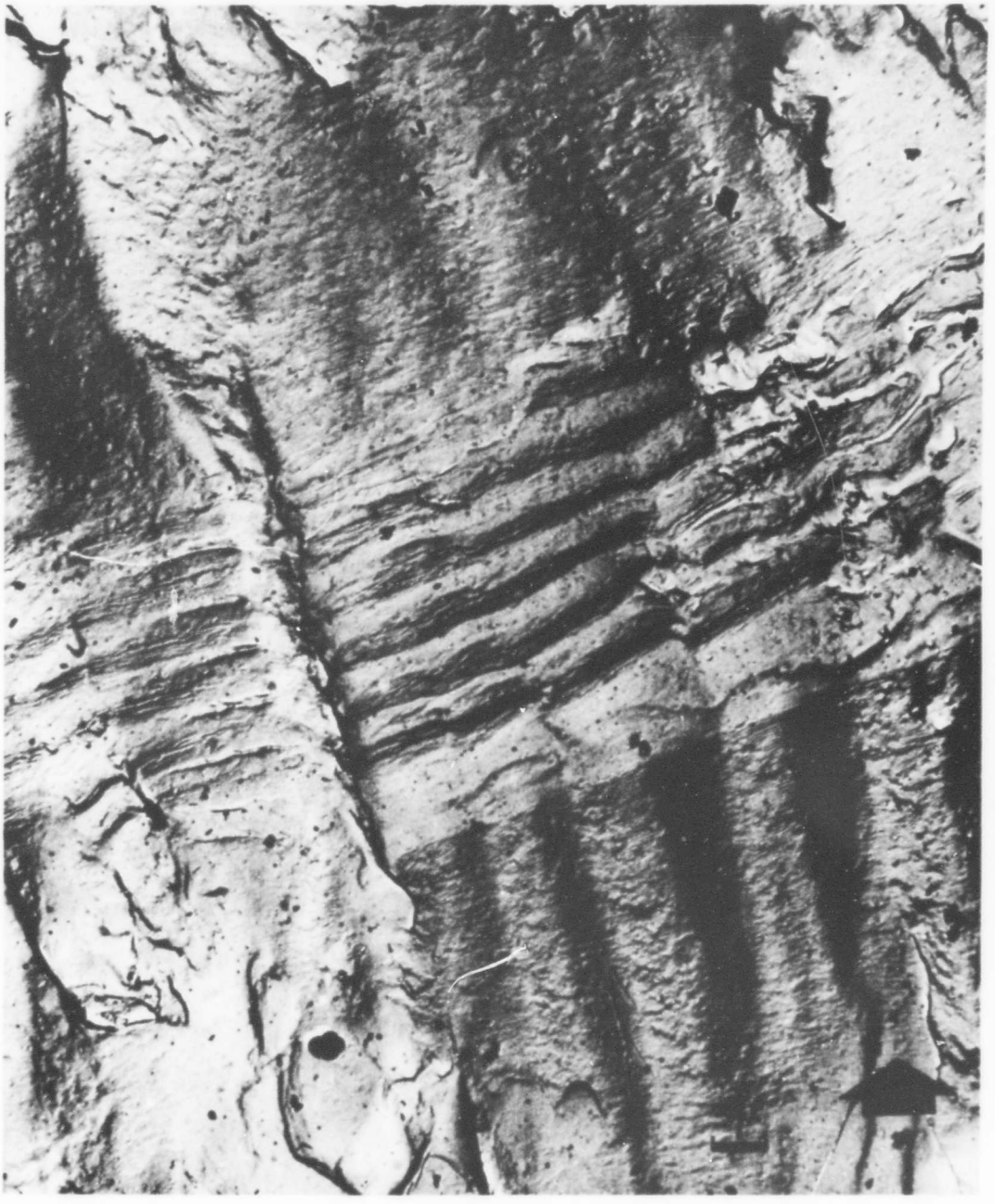

Figure 33b (courtesy of Rutkiewicz and Mavec, Wichita Division) Note the large crack jump occurring on the application of the first large load. The spacing of the first striation is larger than for the following five striations, although the load amplitude and level are the same. Use with Figure 33a to form a stereo image, and note the difference in crack tip profile after 1125 cycles at 18,350 psi and at each of the large load cycles (28,450 psi).

crack tip due to a smaller crack tip radius. The sharpness of the crack tip can be qualitatively observed in Figures 28 and 29, where the ridges of the striations are very sharp. The difference between random and program loading will be more marked at the slower growth rate where the crack tip is much sharper. This was observed by Paris[18] and Smith,[19] who found that random loading is faster than sinusoidal loading for growth rates below $10^{-5}$ or $10^{-4}$ inches/cycle. It should also be mentioned that crack tip blunting under a peak overload may account for part of the crack arrest phenomena. On the other hand, continuous crack tip resharpening in a corrosive medium explains the acceleration of crack growth rates in corrosion fatigue.

In summary, it can be said that the importance of the crack tip radius and the associated stress and strain concentration factors has been underestimated in all the analysis of the mechanisms of fatigue crack propagation. Also, before we can understand the complex fatigue crack propagation behavior of a material under program or random loads it will be necessary to have a better knowledge of the cyclic workhardening which takes place in the plastic zone. Our present work has not given an answer to these two challenging problems. However, we have been able to appraise the important contribution that the techniques of fractography can provide in this field of research. Further tests with higher peak overloads to create larger crack jumps and crack arrest are underway. The number of cycles at a given stress level has been increased markedly in order

to measure changes in rates due to arrest or deceleration. In the long range this type of work is aimed at determining the different parameters which control growth rates in order to establish a set of relationships which can be used first for the analysis, and then for the prediction of cumulative damage.

## V. SUMMARY

In this paper it has been shown that fatigue crack propagation tests under program and random loads, combined with a study of striation counts and spacing measurements by electron microscopy, have given us a better understanding of the mechanisms of fatigue cracking. The main findings with respect to aluminum alloy 2024-T3 are as follows:

1. The advance of the fatigue crack front takes place only during the stress rise portion of a cycle.

2. The profile or sides of a striation are related to the loading and unloading sequence of a load cycle.

3. Microscopic crack growth rates were measured as a function of load amplitudes $\Delta S$ and maximum loads $S_{max}$ and an empirical crack growth rate equation was obtained:

$$\text{crack growth rate} = \text{constant } (\Delta S)^n (S_{max})^m$$

This equation relates the relative growth rates at a given crack length under program loading.

4. In random load programs with constant $S_{max}$, the growth rate is the same as the programmed spectra rates. No sequencing effect is apparent in changes in $\Delta S$ alone.

5. In random load programs with variable $S_{max}$, the crack growth rates were higher than for the equivalent programmed load programs. The importance of the crack tip radius in controlling crack rates for random loads was pointed out.

6. The measured crack growth rate of program and random load crack propagation tests were compared with rates calculated by a computer program. The computed rates are not conservative but they do not differ from the measured rates by a factor of more than two. The application of Miner's rule resulted in $\sum \frac{n}{N}$ values of the order of .650 for the constant maximum load programs and of .850 for the variable maximum load programs.

## REFERENCES


1. *Proceedings of the Crack Propagation Symposium, Cranfield, England, September 1961,* College of Aeronautics, Cranfield, England, 1962.

2. Schijve, J., J. R. Heath-Smith, and E. R. Welbourne (editors), *Current Aeronautical Fatigue Problems: Proceedings of the ICAF Symposium, Rome, April 1963,* Pergamon Press, New York, New York, 1965.

3. *Mechanisms of Fatigue in Crystalline Solids: Proceedings of an International Conference on the Mechanisms of Fatigue in Crystalline Solids, Orlando, Florida, November 1962,* Pergamon Press, New York, New York. Also, *Acta Metallurgica 11,* July 1963.

4. *Fatigue: an interdisciplinary approach - Proceedings of the Tenth Sagamore Army Materials Research Conference, August 1963,* Syracuse University Press, Syracuse, New York, 1964.

5. *ASTM Symposium on Fatigue Crack Propagation, Atlantic City, New Jersey, June 1966* (69th ASTM Annual Meeting), to be published.

6. Zapffe, C. A. and C. Worden, *Trans. ASM 43,* 958, 1951.

7. Pelloux, R. M., *Trans. ASM 57,* 511, 1964.

8. Forsythe, P. and D. Ryder, "Fatigue Fracture," *Aircraft Engineering 32,* 96, April 1960.

9. Hertzberg, R. W., "Application of Electron Fractography and Fracture Mechanics to Fatigue Crack Propagation in High Strength Aluminum Alloys," Ph.D. Dissertation, Lehigh University, Bethlehem, Pennsylvania, 15 May 1965.

10. McMillan, J. C., "Fractographic Analysis of Fatigue Crack Propagation," presented at technical sessions of Fractography Subcommittee of ASTM Committee E-24, Lehigh University, Bethlehem, Pennsylvania, 5 October 1965.

11. Schijve, J., "Fatigue Life and Crack Propagation under Random and Programmed Load Sequences," p. 403, *Current Aeronautical Fatigue Problems,* Pergamon Press, New York, New York, 1965.

12. Forsyth, P.J.E., "Fatigue Damage and Crack Growth in Aluminum Alloys," *Acta Metallurgica 11,* p. 703, July 1963.

13. Laird, C., "Influence of Metallurgical Structures on the Mechanism of Fatigue Crack Propagation," *ASTM Symposium on Fatigue Crack Propagation, Atlantic City, New Jersey, June 1966* (69th ASTM Annual Meeting), to be published.

14. Laird, C. and G. C. Smith, "Crack Propagation in High Stress Fatigue," *Phil. Mag. 7*, 847, 1962.

15. McEvily, A. J. Jr., R. C. Boettner, and T. L. Johnston, "On the Formation and Growth of Fatigue Cracks in Polymers," p. 95, *Fatigue: an interdisciplinary approach - Proceedings of the Tenth Sagamore Army Materials Research Conference, August 1963*, Syracuse University Press, Syracuse, New York, 1964.

16. Schijve, J., *Analysis of the Fatigue Phenomenon in Aluminum Alloys*, NLR Technical Report M2122, April 1964.

17. Viswanathan, N. and R. Plunkett, *Fatigue Crack Propagation Rates Under Random Excitation*, paper to be published, University of Minnesota, Minneapolis, Minnesota.

18. Paris, P. C., "The Fracture Mechanics Approach to Fatigue," p. 107, *Fatigue: an interdisciplinary approach - Proceedings of the Tenth Sagamore Army Materials Research Conference, August 1963*, Syracuse University Press, Syracuse, New York, 1965.

19. Smith, S. H., "Fatigue Crack Growth under Axial Narrow and Broad Band Random Loading," p. 331, *Acoustical Fatigue in Aerospace Structures*, Syracuse University Press, Syracuse, New York, 1965.

20. Hertzberg, R. W., "Fracture Surface Appearance," *ASTM Symposium on Fatigue Crack Propagation, Atlantic City, New Jersey, June 1966* (69th ASTM Annual Meeting), to be published.

21. Hardrath, H. F., "Cumulative Damage," p. 345, *Fatigue: an interdisciplinary approach - Proceedings of the Tenth Sagamore Army Materials Research Conference, August 1963*, Syracuse University Press, Syracuse, New York, 1964.

22. Crews, J. H. and H. F. Hardrath, "A Study of Cyclic Plastic Stresses at a Notch Root," presented at the Society for Experimental Stress Analysis Meeting, Denver, Colorado, May 1965.

## APPENDIX I - TEST DATA

| Program P1 Alloy 7075 T6 | | Program P6 Alloy 7075 T6 | | Program P2 Alloy 7075 T6 | | Program P7 Alloy 7075 T6 | |
|---|---|---|---|---|---|---|---|
| Periods Number N | Crack Length 2a | Periods Number N | Crack Lenght 2a | Periods Number N | Crack Length 2a | Periods Number N | Crack Length 2a |
| 0 | 0.494 | 0 | 0.502 | 0 | 0.539 | 0 | 0.505 |
| 375 | 0.506 | 200 | 0.510 | 200 | 0.549 | 300 | 0.529 |
| 475 | 0.535 | 300 | 0.523 | 506 | 0.594 | 500 | 0.377 |
| 550 | 0.553 | 450 | 0.547 | 750 | 0.619 | 700 | 0.619 |
| 650 | 0.575 | 600 | 0.582 | 1000 | 0.657 | 900 | 0.691 |
| 750 | 0.599 | 750 | 0.624 | 1250 | 0.663 | 1100 | 0.765 |
| 850 | 0.645 | 900 | 0.652 | 1500 | 0.734 | 1300 | 0.849 |
| 950 | 0.673 | 1050 | 0.692 | 1750 | 0.811 | 1500 | 0.956 |
| 1100 | 0.756 | 1200 | 0.733 | 2050 | 0.946 | 1720 | 1.076 |
| 1250 | 0.828 | 1400 | 0.790 | 2300 | 1.072 | 1900 | 1.198 |
| 1400 | 0.912 | 1600 | 0.855 | 2550 | 1.163 | 2100 | 1.418 |
| 1550 | 0.990 | 1820 | 0.941 | 2750 | 1.366 | 2200 | 1.529 |
| 1700 | 1.124 | 2000 | 1.028 | 2850 | 1.455 | 2350 | 1.814 |
| 1850 | 1.256 | 2150 | 1.118 | 2952 | 1.561 | 2400 | 1.986 |
| 1950 | 1.365 | 2250 | 1.170 | 3100 | 1.724 | 2450 | 2.268 |
| 2050 | 1.492 | 2400 | 1.230 | 3250 | 1.896 | 2499 | |
| 2150 | 1.649 | 2550 | 1.457 | 3500 | 2.248 | | |
| 2250 | 1.818 | 2650 | 1.484 | 3600 | 2.432 | | |
| 2350 | 2.063 | 2700 | 1.547 | 3750 | 2.700 | | |
| 2450 | 2.318 | 2800 | 1.592 | 3850 | 3.042 | | |
| 2550 | 2.686 | 2900 | 1.691 | 3950 | 3.686 | | |
| 2600 | 2.923 | 3000 | 1.821 | 3981 | | | |
| 2650 | 3.254 | 3100 | 2.011 | | | | |
| 2700 | 4.080 | 3150 | 2.133 | | | | |
| 2712 | | 3200 | 2.280 | | | | |
| | | 3225 | 2.431 | | | | |
| | | 3250 | 2.573 | | | | |
| | | 3275 | 2.718 | | | | |
| | | 3300 | 2.942 | | | | |
| | | 3315 | | | | | |

| Program P1 Alloy 2024 T3 | | | Program P2 Alloy 2024 T3 | | Program P3 Alloy 2024 T3 | | Program P4 Alloy 2024 T3 | |
|---|---|---|---|---|---|---|---|---|
| Periods Number N | Crack Length 2a | | Periods Number N | Crack Length 2a | Periods Number N | Crack Length 2a | Periods Number N | Crack Length 2a |
| 0 | 0,498 | 0,249 | 0 | 0.509 | 0 | 0.492 | 0 | 0.521 |
| 250 | 0.517 | 0.258 | 500 | 0.537 | 250 | 0.502 | 125 | 0.530 |
| 600 | 0,566 | 0.283 | 1125 | 0.643 | 500 | 0.555 | 200 | 0.545 |
| 1000 | 0.628 | 0.314 | 1750 | 0.833 | 600 | 0.589 | 275 | 0.568 |
| 1600 | 0.764 | 0.382 | 2300 | 0.982 | 750 | 0.643 | 350 | 0.586 |
| 2000 | 0.914 | 0.457 | 2750 | 1.149 | 900 | 0.684 | 475 | 0.654 |
| 2500 | 1,110 | 0.550 | 3550 | 1.540 | 1050 | 0.730 | 550 | 0.702 |
| 3100 | 1,466 | 0.733 | 4000 | 1.933 | 1200 | 0.798 | 650 | 0.778 |
| 3500 | 1,784 | 0.892 | 4500 | 2.548 | 1400 | 0.886 | 750 | 0.865 |
| 4100 | 2,479 | 1.240 | 5000 | 3.642 | 1600 | 0.983 | 850 | 0.958 |
| 4400 | 3,001 | 1,500 | 5250 | 4.80 | 1850 | 1.121 | 950 | 1.070 |
| 4500 | 3,233 | 1,616 | 5300 | 5.27 | 2050 | 1.279 | 1050 | 1.203 |
| 4750 | 4,051 | 2,025 | 5325 | 5.55 | 2175 | 1.371 | 1150 | 1.346 |
| 4850 | 4,646 | 2,323 | 5355 | 6.40 | 2275 | 1.467 | 1225 | 1.479 |
| 4925 | 5,326 | 2,663 | 5360 | | 2375 | 1.573 | 1375 | 1.789 |
| 4940 | 5,75 | 2,87 | | | 2475 | 1.655 | 1400 | 1.855 |
| 4945 | 5,85 | 2,92 | | | 2600 | 1.800 | 1475 | 2.063 |
| 4950 | 6,00 | 3,00 | | | 2700 | 1.916 | 1550 | 2.303 |
| 4955 | | | | | 2800 | 2.050 | 1600 | 2.519 |
| | | | | | 2900 | 2.206 | 1650 | 2.751 |
| | | | | | 3000 | 2.386 | 1700 | 3.020 |
| | | | | | 3125 | 2.650 | 1750 | 3.389 |
| | | | | | 3200 | 2.830 | 1800 | 3.87 |
| | | | | | 3300 | 3.128 | 1825 | 4.18 |
| | | | | | 3400 | 3.490 | 1850 | 4.63 |
| | | | | | 3450 | 3.77 | 1875 | 5.42 |
| | | | | | 3550 | 4.50 | | |
| | | | | | 3575 | 4.80 | | |
| | | | | | 3590 | 5.00 | | |
| | | | | | 3595 | 5.08 | | |
| | | | | | 3600 | 5.18 | | |
| | | | | | 3605 | 5.26 | | |
| | | | | | 3610 | 5.37 | | |
| | | | | | 3615 | 5.48 | | |
| | | | | | 3620 | 5.59 | | |
| | | | | | 3625 | 5.77 | | |
| | | | | | 3630 | 5.95 | | |
| | | | | | 3635 | 6.33 | | |
| | | | | | 3639 | Failed | | |

| Program P5 Alloy 2024 T3 | | Program P6 Alloy 2024 T3 | | Program P7 Alloy 2024 T3 | | Program P8 Alloy 2024 T3 | |
|---|---|---|---|---|---|---|---|
| Periods Number N | Crack Length 2a | Periods Number N | Cracks Length 2a | Periods Number N | Crack Length 2a | Periods Number N | Crack Length 2a |
| 0 | 0.512 | 0 | 0.513 | 0 | 0.501 | 0 | 0.5254 |
| 350 | 0.529 | 500 | 0.524 | 900 | 0.531 | 300 | 0.5574 |
| 450 | 0.552 | 1000 | 0.550 | 1200 | 0.547 | 650 | 0.637 |
| 650 | 0.596 | 1600 | 0.602 | 1600 | 0.582 | 1000 | 0.729 |
| 775 | 0.627 | 2000 | 0.618 | 2000 | 0.620 | 1375 | 0.859 |
| 910 | 0.677 | 2500 | 0.672 | 2450 | 0.664 | 1700 | 0.993 |
| 1050 | 0.716 | 3000 | 0.733 | 2900 | 0.719 | 1975 | 1.131 |
| 1200 | 0.775 | 3500 | 0.807 | 3500 | 0.804 | 2250 | 1.312 |
| 1350 | 0.831 | 4000 | 0.876 | 4118 | 0.907 | 2500 | 1.534 |
| 1550 | 0.941 | 4500 | 0.975 | 4500 | 0.951 | 2775 | 1.817 |
| 1710 | 1.025 | 5000 | 1.077 | 5400 | 1.120 | 3000 | 2.123 |
| 1850 | 1.104 | 5500 | 1.184 | 5800 | 1.184 | 3200 | 2.460 |
| 2000 | 1.203 | 6000 | 1.318 | 6307 | 1.295 | 3300 | 2.687 |
| 2100 | 1.287 | 6750 | 1.539 | 6800 | 1.444 | 3400 | 2.882 |
| 2200 | 1.358 | 7500 | 1.817 | 7300 | 1.569 | 3550 | 3.35 |
| 2325 | 1.473 | 8100 | 2.083 | 7700 | 1.718 | 3650 | 3.75 |
| 2450 | 1.592 | 8600 | 2.383 | 8000 | 1.835 | 3725 | 4.13 |
| 2560 | 1.722 | 9200 | 2.798 | 8300 | 1.958 | 3750 | 4.29 |
| 2650 | 1.843 | 9800 | 3.426 | 8600 | 2.072 | 3775 | 4.47 |
| 2775 | 2.010 | 10125 | 3.821 | 9400 | 2.475 | 3800 | 4.77 |
| 2875 | 2.177 | 10250 | 4.036 | 9800 | 2.650 | 3815 | 5.02 |
| 3000 | 2.417 | 10300 | 4.16 | 10000 | 2.818 | 3830 | 5.20 |
| 3100 | 2.650 | 10350 | 4.24 | 10200 | 2.956 | 3840 | 5.45 |
| 3150 | 2.780 | 10450 | 4.48 | 10400 | 3.122 | 3850 | 5.70 |
| 3200 | 2.920 | 10525 | 4.71 | 10600 | 3.299 | 3860 | 5.92 |
| 3250 | 3.093 | 10650 | 5.12 | 10800 | 3.466 | 3867 | |
| 3310 | 3.310 | 10675 | 5.25 | 11000 | 3.684 | | |
| 3350 | 3.479 | 10700 | 5.37 | 11200 | 3.925 | | |
| 3400 | 3.750 | 10725 | 5.55 | 11405 | 4.245 | | |
| 3425 | 3.880 | 10750 | 5.74 | 11600 | 4.588 | | |
| 3450 | 4.020 | 10775 | 6.04 | 11900 | 5.722 | | |
| 3475 | 4.180 | 10780 | 6.14 | 11921 | | | |
| 3500 | 4.350 | 10785 | 6.24 | | | | |
| 3525 | 4.620 | 10790 | | | | | |
| 3540 | 4.750 | | | | | | |
| 3570 | 5.150 | | | | | | |
| 3580 | 5.320 | | | | | | |
| 3590 | 5.520 | | | | | | |
| 3600 | 5.800 | | | | | | |
| 3605 | 6.010 | | | | | | |
| 3610 | 6.270 | | | | | | |
| 3613 | | | | | | | |

| Program P9 Alloy 2024 T3 | | Program P10 Alloy 2024 T3 | | Program P11 Alloy 2024 T3 | | Program P12 Alloy 2024 T3 | |
|---|---|---|---|---|---|---|---|
| Periods Number N | Crack Length 2a | Periods Number N | Crack Length 2a | Periods Number N | Crack Length 2a | Periods Number N | Crack Length 2a |
| 0 | 0.499 | 0 | 0.511 | 0 | 0.505 | 0 | 0.492 |
| 250 | 0.525 | 150 | 0.524 | 250 | 0.513 | 400 | 0.505 |
| 500 | 0.572 | 300 | 0.567 | 500 | 0.519 | 800 | 0.585 |
| 750 | 0.643 | 500 | 0.622 | 750 | 0.525 | 1125 | 0.626 |
| 1000 | 0.723 | 700 | 0.713 | 1000 | 0.543 | 1725 | 0.762 |
| 1250 | 0.823 | 950 | 0.845 | 1250 | 0.570 | 1825 | 0.785 |
| 1500 | 0.931 | 1125 | 0.967 | 1500 | 0.592 | 2000 | 0.848 |
| 1750 | 1.066 | 1250 | 1.050 | 1750 | 0.620 | 2250 | 0.930 |
| 2000 | 1.240 | 1400 | 1.189 | 2000 | 0.648 | 2400 | 0.977 |
| 2250 | 1.438 | 1550 | 1.380 | 2200 | 0.675 | 2600 | 1.070 |
| 2600 | 1.792 | 1700 | 1.573 | 2500 | 0.722 | 2925 | 1.230 |
| 2800 | 2.077 | 1900 | 1.878 | 2750 | 0.751 | 3250 | 1.417 |
| 3000 | 2.382 | 2110 | 2.322 | 3100 | 0.815 | 3525 | 1.636 |
| 3208 | 2.819 | 2275 | 2.844 | 3400 | 0.870 | 3850 | 1.921 |
| 3303 | 3.072 | 2400 | 3.50 | 3700 | 0.941 | 4100 | 2.210 |
| 3406 | 3.402 | 2520 | 4.73 | 4050 | 1.023 | 4350 | 2.575 |
| 3452 | 3.600 | 2553 | | 4350 | 1.108 | 4500 | 2.859 |
| 3504 | 3.88 | | | 4700 | 1.239 | 4625 | 3.19 |
| 3575 | 4.28 | | | 5050 | 1.329 | 4700 | 3.38 |
| 3625 | 4.70 | | | 5500 | 1.508 | 4800 | 3.71 |
| 3675 | 5.37 | | | 5900 | 1.700 | 4900 | 4.18 |
| 3700 | Failed | | | 6200 | 1.858 | 5000 | 4.90 |
| | | | | 6500 | 2.039 | 5025 | 5.20 |
| | | | | 6950 | 2.372 | 5050 | 5.62 |
| | | | | 7200 | 2.585 | 5070 | 6.30 |
| | | | | 7900 | 2.893 | | |

Program P13
Alloy 2024 T3

| Periods Number N | Crack Length 2a |
|---|---|
| 0 | 0.504 |
| 300 | 0.511 |
| 600 | 0.592 |
| 700 | 0.626 |
| 850 | 0.674 |
| 1000 | 0.760 |
| 1175 | 0.815 |
| 1400 | 0.961 |
| 1605 | 1.070 |
| 1800 | 1.225 |
| 1925 | 1.335 |
| 2075 | 1.480 |
| 2200 | 1.623 |
| 2350 | 1.825 |
| 2450 | 1.976 |
| 2605 | 2.247 |
| 2680 | 2.405 |

## APPENDIX II - COMPUTER PROGRAMS

PROGRAM P1 CRACK GROWTH IN 2024 T3 PANELS

FOR THIS SET OF CONDITIONS,

THE NUMBER OF FLIGHTS TAKEN IS 7968

THE CRACK LENGTH REACHED IS 3.27102 INCHES

THE CONTROL CRACK LENGTH SPECIFIED IS 3.25000 INCHES

| FLIGHT, | CRACK LENGTH | FLIGHT | CRACK LENGTH |
|---|---|---|---|
| 159 | 0.255001 | 4293 | 0.515707 |
| 318 | 0.260228 | 4452 | 0.534070 |
| 477 | 0.265695 | 4611 | 0.553572 |
| 636 | 0.271416 | 4770 | 0.574308 |
| 795 | 0.277408 | 4929 | 0.596378 |
| 954 | 0.283688 | 5088 | 0.619890 |
| 1113 | 0.290276 | 5247 | 0.644876 |
| 1272 | 0.297201 | 5406 | 0.671515 |
| 1431 | 0.304488 | 5565 | 0.700916 |
| 1590 | 0.312144 | 5724 | 0.732789 |
| 1749 | 0.320192 | 5883 | 0.767326 |
| 1908 | 0.328652 | 6042 | 0.804890 |
| 2067 | 0.337545 | 6201 | 0.845348 |
| 2226 | 0.346890 | 6360 | 0.889468 |
| 2385 | 0.356708 | 6519 | 0.938342 |
| 2544 | 0.367015 | 6678 | 0.993105 |
| 2703 | 0.377825 | 6837 | 1.055434 |
| 2862 | 0.389151 | 6996 | 1.128334 |
| 3021 | 0.400710 | 7155 | 1.217298 |
| 3180 | 0.412714 | 7314 | 1.327602 |
| 3339 | 0.425281 | 7473 | 1.470291 |
| 3498 | 0.438459 | 7632 | 1.668310 |
| 3657 | 0.452299 | 7791 | 1.990210 |
| 3816 | 0.466860 | 7950 | 2.887476 |
| 3975 | 0.482211 | 7968 | 3.271015 |
| 4134 | 0.498429 | | |

PROGRAM P2 CRACK GROWTH IN 2024 T3 PANELS

FOR THIS SET OF CONDITIONS,

THE NUMBER OF FLIGHTS TAKEN IS 7968

THE CRACK LENGTH REACHED IS 3.26254 INCHES

THE CONTROL CRACK LENGTH SPECIFIED IS 3.25000 INCHES

| FLIGHT. | CRACK LENGTH | FLIGHT | CRACK LENGTH |
|---|---|---|---|
| 159 | 0.255002 | 4293 | 0.515720 |
| 318 | 0.260229 | 4452 | 0.534084 |
| 477 | 0.265695 | 4611 | 0.553587 |
| 636 | 0.271417 | 4770 | 0.574324 |
| 795 | 0.277409 | 4929 | 0.596395 |
| 954 | 0.283690 | 5088 | 0.619909 |
| 1113 | 0.290278 | 5247 | 0.644895 |
| 1272 | 0.297204 | 5406 | 0.671535 |
| 1431 | 0.304491 | 5565 | 0.700939 |
| 1590 | 0.312148 | 5724 | 0.732814 |
| 1749 | 0.320197 | 5883 | 0.767353 |
| 1908 | 0.328657 | 6042 | 0.804918 |
| 2067 | 0.337550 | 6201 | 0.845379 |
| 2226 | 0.346896 | 6360 | 0.889501 |
| 2385 | 0.356715 | 6519 | 0.938378 |
| 2544 | 0.367022 | 6678 | 0.993142 |
| 2703 | 0.377833 | 6837 | 1.055470 |
| 2862 | 0.389159 | 6996 | 1.128352 |
| 3021 | 0.400718 | 7155 | 1.217305 |
| 3180 | 0.412722 | 7314 | 1.327593 |
| 3339 | 0.425291 | 7473 | 1.470257 |
| 3498 | 0.438468 | 7632 | 1.668215 |
| 3657 | 0.452309 | 7791 | 1.989930 |
| 3816 | 0.466871 | 7950 | 2.884441 |
| 3975 | 0.482223 | 7968 | 3.262541 |
| 4134 | 0.498441 | | |

PROGRAM P3 CRACK GROWTH IN 2024 T3 PANELS

FOR THIS SET OF CONDITIONS,

THE NUMBER OF FLIGHTS TAKEN IS 5526

THE CRACK LENGTH REACHED IS 3.26622 INCHES

THE CONTROL CRACK LENGTH SPECIFIED IS 3.25000 INCHES

| FLIGHT, | CRACK LENGTH | FLIGHT | CRACK LENGTH |
|---|---|---|---|
| 111 | 0.254990 | 2886 | 0.498631 |
| 222 | 0.260203 | 2997 | 0.516248 |
| 333 | 0.265653 | 3108 | 0.534999 |
| 444 | 0.271354 | 3219 | 0.554954 |
| 555 | 0.277323 | 3330 | 0.576216 |
| 666 | 0.283575 | 3441 | 0.598894 |
| 777 | 0.290129 | 3552 | 0.623108 |
| 888 | 0.297006 | 3663 | 0.648890 |
| 999 | 0.304226 | 3774 | 0.676511 |
| 1110 | 0.311808 | 3885 | 0.707173 |
| 1221 | 0.319773 | 3996 | 0.740365 |
| 1332 | 0.328144 | 4107 | 0.776412 |
| 1443 | 0.336942 | 4218 | 0.815694 |
| 1554 | 0.346191 | 4329 | 0.857720 |
| 1665 | 0.355912 | 4440 | 0.903897 |
| 1776 | 0.366126 | 4551 | 0.955213 |
| 1887 | 0.376854 | 4662 | 1.012947 |
| 1998 | 0.388113 | 4773 | 1.079113 |
| 2109 | 0.399705 | 4884 | 1.157810 |
| 2220 | 0.411762 | 4995 | 1.254227 |
| 2331 | 0.424416 | 5106 | 1.375048 |
| 2442 | 0.437718 | 5217 | 1.533539 |
| 2553 | 0.451723 | 5328 | 1.760944 |
| 2664 | 0.466495 | 5439 | 2.165308 |
| 2775 | 0.482104 | 5526 | 3.266218 |

PROGRAM P5 CRACK GROWTH IN 2024 T3 PANELS

FOR THIS SET OF CONDITIONS,

THE NUMBER OF FLIGHTS TAKEN IS 5526

THE CRACK LENGTH REACHED IS 3.25610 INCHES

THE CONTROL CRACK LENGTH SPECIFIED IS 3.25000 INCHES

| FLIGHT, | CRACK LENGTH | FLIGHT | CRACK LENGTH |
|---|---|---|---|
| 110 | 0.254943 | 2970 | 0.511694 |
| 220 | 0.260104 | 3080 | 0.529981 |
| 330 | 0.265496 | 3190 | 0.549423 |
| 440 | 0.271134 | 3300 | 0.570120 |
| 550 | 0.277034 | 3410 | 0.592178 |
| 660 | 0.283211 | 3520 | 0.615708 |
| 770 | 0.289684 | 3630 | 0.640774 |
| 880 | 0.296472 | 3740 | 0.667515 |
| 990 | 0.303595 | 3850 | 0.696911 |
| 1100 | 0.311073 | 3960 | 0.728938 |
| 1210 | 0.318924 | 4070 | 0.763656 |
| 1320 | 0.327172 | 4180 | 0.801417 |
| 1430 | 0.335836 | 4290 | 0.842060 |
| 1540 | 0.344941 | 4400 | 0.886198 |
| 1650 | 0.354505 | 4510 | 0.935012 |
| 1760 | 0.364552 | 4620 | 0.989602 |
| 1870 | 0.375099 | 4730 | 1.051578 |
| 1980 | 0.386165 | 4840 | 1.123748 |
| 2090 | 0.397608 | 4950 | 1.211695 |
| 2200 | 0.409449 | 5060 | 1.320150 |
| 2310 | 0.421868 | 5170 | 1.459127 |
| 2420 | 0.434913 | 5280 | 1.648398 |
| 2530 | 0.448637 | 5390 | 1.946119 |
| 2640 | 0.463100 | 5500 | 2.661111 |
| 2750 | 0.478369 | 5526 | 3.256102 |
| 2960 | 0.494519 | | |

PROGRAM P6 CRACK GROWTH IN 2024 T3 PANELS

FOR THIS SET OF CONDITIONS,

THE NUMBER OF FLIGHTS TAKEN IS 12151

THE CRACK LENGTH REACHED IS 2.90380 INCHES

THE CONTROL CRACK LENGTH SPECIFIED IS 2.90000 INCHES

| FLIGHT, | CRACK LENGTH | FLIGHT | CRACK LENGTH |
|---|---|---|---|
| 243 | 0.254394 | 6561 | 0.485921 |
| 486 | 0.258963 | 6804 | 0.504106 |
| 729 | 0.263717 | 7047 | 0.523605 |
| 972 | 0.268665 | 7290 | 0.544562 |
| 1215 | 0.273822 | 7533 | 0.567085 |
| 1458 | 0.279201 | 7776 | 0.591191 |
| 1701 | 0.284816 | 8019 | 0.617153 |
| 1944 | 0.290670 | 8262 | 0.644787 |
| 2187 | 0.296788 | 8505 | 0.674525 |
| 2430 | 0.303200 | 8748 | 0.707847 |
| 2673 | 0.309892 | 8991 | 0.744386 |
| 2916 | 0.316911 | 9234 | 0.784597 |
| 3159 | 0.324283 | 9477 | 0.829064 |
| 3402 | 0.332033 | 9720 | 0.878628 |
| 3645 | 0.340191 | 9963 | 0.934171 |
| 3888 | 0.348790 | 10206 | 0.997013 |
| 4131 | 0.357865 | 10449 | 1.068944 |
| 4374 | 0.367455 | 10692 | 1.152425 |
| 4617 | 0.377588 | 10935 | 1.251246 |
| 4860 | 0.388321 | 11178 | 1.371102 |
| 5103 | 0.399700 | 11421 | 1.522059 |
| 5346 | 0.411789 | 11664 | 1.725326 |
| 5589 | 0.424669 | 11907 | 2.045630 |
| 5832 | 0.439460 | 12150 | 2.895330 |
| 6075 | 0.453198 | 12151 | 2.903804 |
| 6318 | 0.468979 | | |

PROGRAM P7 CRACK GROWTH IN 2024 T3 PANELS

FOR THIS SET OF CONDITIONS,

THE NUMBER OF FLIGHTS TAKEN IS 13517

THE CRACK LENGTH REACHED IS 2.90526 INCHES

THE CONTROL CRACK LENGTH SPECIFIED IS 2.90000 INCHES

| FLIGHT, | CRACK LENGTH | FLIGHT | CRACK LENGTH |
|---|---|---|---|
| 270 | 0.254257 | 7290 | 0.493558 |
| 540 | 0.258693 | 7560 | 0.513151 |
| 810 | 0.263320 | 7830 | 0.534234 |
| 1080 | 0.268149 | 8100 | 0.556961 |
| 1350 | 0.273196 | 8370 | 0.581319 |
| 1620 | 0.278477 | 8640 | 0.607525 |
| 1890 | 0.284008 | 8910 | 0.635692 |
| 2160 | 0.289811 | 9180 | 0.665994 |
| 2430 | 0.295918 | 9450 | 0.699478 |
| 2700 | 0.302353 | 9720 | 0.736427 |
| 2970 | 0.309092 | 9990 | 0.776953 |
| 3240 | 0.316189 | 10260 | 0.821518 |
| 3510 | 0.323673 | 10530 | 0.870501 |
| 3780 | 0.331576 | 10800 | 0.924568 |
| 4050 | 0.339931 | 11070 | 0.984756 |
| 4320 | 0.348774 | 11340 | 1.052260 |
| 4590 | 0.358148 | 11610 | 1.128636 |
| 4860 | 0.368094 | 11880 | 1.216141 |
| 5130 | 0.378623 | 12150 | 1.317953 |
| 5400 | 0.389821 | 12420 | 1.438771 |
| 5670 | 0.401735 | 12690 | 1.587177 |
| 5940 | 0.414448 | 12960 | 1.782270 |
| 6210 | 0.428071 | 13230 | 2.082376 |
| 6480 | 0.442718 | 13500 | 2.801352 |
| 6750 | 0.458439 | 13517 | 2.905261 |
| 7020 | 0.475339 | | |

PROGRAM P8 CRACK GROWTH IN 2024 T3 PANELS

FOR THIS SET OF CONDITIONS,

THE NUMBER OF FLIGHTS TAKEN IS 4440

THE CRACK LENGTH REACHED IS 2.90840 INCHES

THE CONTROL CRACK LENGTH SPECIFIED IS 2.90000 INCHES

| FLIGHT, | CRACK LENGTH | FLIGHT | CRACK LENGTH |
|---|---|---|---|
| 89 | 0.254570 | 2314 | 0.492571 |
| 178 | 0.259339 | 2403 | 0.511530 |
| 267 | 0.264321 | 2492 | 0.531782 |
| 356 | 0.269529 | 2581 | 0.553454 |
| 445 | 0.274980 | 2670 | 0.576589 |
| 534 | 0.280692 | 2759 | 0.601304 |
| 623 | 0.286682 | 2848 | 0.627685 |
| 712 | 0.292975 | 2937 | 0.655711 |
| 801 | 0.299612 | 3026 | 0.686175 |
| 890 | 0.306586 | 3115 | 0.719826 |
| 979 | 0.313922 | 3204 | 0.756426 |
| 1068 | 0.321654 | 3293 | 0.796337 |
| 1157 | 0.329814 | 3382 | 0.839929 |
| 1246 | 0.338431 | 3471 | 0.887543 |
| 1335 | 0.347540 | 3560 | 0.940017 |
| 1424 | 0.357176 | 3649 | 0.998263 |
| 1513 | 0.367377 | 3738 | 1.063474 |
| 1602 | 0.378128 | 3827 | 1.137188 |
| 1691 | 0.389513 | 3916 | 1.221763 |
| 1780 | 0.401578 | 4005 | 1.320636 |
| 1869 | 0.414397 | 4094 | 1.439226 |
| 1958 | 0.428055 | 4183 | 1.588485 |
| 2047 | 0.442640 | 4272 | 1.792941 |
| 2136 | 0.458201 | 4361 | 2.127930 |
| 2225 | 0.474816 | 4440 | 2.908402 |

PROGRAM. P9 CRACK GROWTH IN 2024 T3 PANELS

FOR THIS SET OF CONDITIONS,

THE NUMBER OF FLIGHTS TAKEN IS 4466

THE CRACK LENGTH REACHED IS 2.90974 INCHES

THE CONTROL CRACK LENGTH SPECIFIED IS 2.90000 INCHES

| FLIGHT, | CRACK LENGTH | FLIGHT | CRACK LENGTH |
|---|---|---|---|
| 89 | 0.254548 | 2403 | 0.510838 |
| 178 | 0.259296 | 2492 | 0.530969 |
| 267 | 0.264256 | 2581 | 0.552501 |
| 356 | 0.269443 | 2670 | 0.575478 |
| 445 | 0.274874 | 2759 | 0.600005 |
| 534 | 0.280566 | 2848 | 0.626183 |
| 623 | 0.286538 | 2937 | 0.653969 |
| 712 | 0.292819 | 3026 | 0.684080 |
| 801 | 0.299448 | 3115 | 0.717364 |
| 890 | 0.306419 | 3204 | 0.753528 |
| 979 | 0.313753 | 3293 | 0.792911 |
| 1068 | 0.321486 | 3382 | 0.835869 |
| 1157 | 0.329647 | 3471 | 0.882696 |
| 1246 | 0.338268 | 3560 | 0.934154 |
| 1335 | 0.347382 | 3649 | 0.991080 |
| 1424 | 0.357022 | 3738 | 1.054546 |
| 1513 | 0.367226 | 3827 | 1.125833 |
| 1602 | 0.377970 | 3916 | 1.206865 |
| 1691 | 0.389341 | 4005 | 1.300736 |
| 1780 | 0.401377 | 4094 | 1.412004 |
| 1869 | 0.414154 | 4183 | 1.549582 |
| 1958 | 0.427760 | 4272 | 1.733445 |
| 2047 | 0.442284 | 4361 | 2.013495 |
| 2136 | 0.457773 | 4450 | 2.642915 |
| 2225 | 0.474312 | 4466 | 2.909745 |
| 2314 | 0.491979 | | |

PROGRAM P11 CRACK GROWTH IN 2024 T3 PANELS

FOR THIS SET OF CONDITIONS,

THE NUMBER OF FLIGHTS TAKEN IS 9741

THE CRACK LENGTH REACHED IS 2.90281 INCHES

THE CONTROL CRACK LENGTH SPECIFIED IS 2.90000 INCHES

| FLIGHT, | CRACK LENGTH | FLIGHT | CRACK LENGTH |
|---|---|---|---|
| 195 | 0.254486 | 5070 | 0.492681 |
| 390 | 0.259166 | 5265 | 0.511706 |
| 585 | 0.264053 | 5460 | 0.531950 |
| 780 | 0.269163 | 5655 | 0.553602 |
| 975 | 0.274512 | 5850 | 0.576788 |
| 1170 | 0.280117 | 6045 | 0.601645 |
| 1365 | 0.285998 | 6240 | 0.628270 |
| 1560 | 0.292174 | 6435 | 0.656700 |
| 1755 | 0.298719 | 6630 | 0.687700 |
| 1950 | 0.305635 | 6825 | 0.721946 |
| 2145 | 0.312930 | 7020 | 0.759219 |
| 2340 | 0.320634 | 7215 | 0.799912 |
| 2535 | 0.328778 | 7410 | 0.844277 |
| 2730 | 0.337395 | 7605 | 0.892808 |
| 2925 | 0.346520 | 7800 | 0.946437 |
| 3120 | 0.356192 | 7995 | 1.006084 |
| 3315 | 0.366451 | 8190 | 1.073019 |
| 3510 | 0.377303 | 8385 | 1.149018 |
| 3705 | 0.388815 | 8580 | 1.236414 |
| 3900 | 0.400998 | 8775 | 1.338075 |
| 4095 | 0.413938 | 8970 | 1.458038 |
| 4290 | 0.427715 | 9165 | 1.603785 |
| 4485 | 0.442399 | 9360 | 1.797256 |
| 4680 | 0.458063 | 9555 | 2.111245 |
| 4875 | 0.474801 | 9741 | 2.902808 |

PROGRAM P12 CRACK GROWTH IN 2024 T3 PANELS

FOR THIS SET OF CONDITIONS,

THE NUMBER OF FLIGHTS TAKEN IS 6942

THE CRACK LENGTH REACHED IS 2.90175 INCHES

THE CONTROL CRACK LENGTH SPECIFIED IS 2.90000 INCHES

| FLIGHT, | CRACK LENGTH | FLIGHT | CRACK LENGTH |
|---|---|---|---|
| 139 | 0.254758 | 3614 | 0.502688 |
| 278 | 0.259730 | 3753 | 0.522007 |
| 417 | 0.264931 | 3892 | 0.542628 |
| 556 | 0.270376 | 4031 | 0.564654 |
| 695 | 0.276084 | 4170 | 0.588189 |
| 834 | 0.282072 | 4309 | 0.613341 |
| 973 | 0.288362 | 4448 | 0.639793 |
| 1112 | 0.294994 | 4587 | 0.667934 |
| 1251 | 0.301979 | 4726 | 0.698832 |
| 1390 | 0.309335 | 4865 | 0.732413 |
| 1529 | 0.317089 | 5004 | 0.768759 |
| 1668 | 0.325267 | 5143 | 0.808208 |
| 1807 | 0.333898 | 5282 | 0.851061 |
| 1946 | 0.343011 | 5421 | 0.897687 |
| 2085 | 0.352636 | 5560 | 0.948859 |
| 2224 | 0.362805 | 5699 | 1.005336 |
| 2363 | 0.373497 | 5838 | 1.068157 |
| 2502 | 0.384719 | 5977 | 1.138275 |
| 2641 | 0.396583 | 6116 | 1.217803 |
| 2780 | 0.409140 | 6255 | 1.310178 |
| 2919 | 0.422450 | 6394 | 1.420749 |
| 3058 | 0.436575 | 6533 | 1.562275 |
| 3197 | 0.451584 | 6672 | 1.762242 |
| 3336 | 0.467552 | 6811 | 2.086557 |
| 3475 | 0.484560 | 6942 | 2.901749 |

PROGRAM P1 CRACK GROWTH IN 7075 T6 PANELS

FOR THIS SET OF CONDITIONS,

THE NUMBER OF FLIGHTS TAKEN IS 5623

THE CRACK LENGTH REACHED IS 2.50277 INCHES

THE CONTROL CRACK LENGTH SPECIFIED IS 2.50000 INCHES

| FLIGHT, | CRACK LENGTH | FLIGHT | CRACK LENGTH |
|---|---|---|---|
| 112 | 0.255822 | 3024 | 0.539007 |
| 224 | 0.261876 | 3136 | 0.559019 |
| 336 | 0.268170 | 3248 | 0.580283 |
| 448 | 0.274720 | 3360 | 0.602909 |
| 560 | 0.281538 | 3472 | 0.627018 |
| 672 | 0.288640 | 3584 | 0.652744 |
| 784 | 0.296039 | 3696 | 0.680402 |
| 896 | 0.303753 | 3808 | 0.710873 |
| 1008 | 0.311797 | 3920 | 0.743711 |
| 1120 | 0.320190 | 4032 | 0.779159 |
| 1232 | 0.328950 | 4144 | 0.816727 |
| 1344 | 0.338096 | 4256 | 0.857094 |
| 1456 | 0.347647 | 4368 | 0.900998 |
| 1568 | 0.357625 | 4480 | 0.948999 |
| 1680 | 0.367948 | 4592 | 1.001794 |
| 1792 | 0.378685 | 4704 | 1.060311 |
| 1904 | 0.389914 | 4816 | 1.125767 |
| 2016 | 0.401671 | 4928 | 1.200275 |
| 2128 | 0.413993 | 5040 | 1.286828 |
| 2240 | 0.426922 | 5152 | 1.390317 |
| 2352 | 0.440504 | 5264 | 1.520710 |
| 2464 | 0.454790 | 5376 | 1.694984 |
| 2576 | 0.469835 | 5488 | 1.955872 |
| 2688 | 0.485701 | 5600 | 2.376551 |
| 2800 | 0.502456 | 5623 | 2.502770 |
| 2912 | 0.520177 | | |

PROGRAM P2  CRACK GROWTH IN 7075 T6 PANELS

FOR THIS SET OF CONDITIONS,

THE NUMBER OF FLIGHTS TAKEN IS  5623

THE CRACK LENGTH REACHED IS  2.50147 INCHES

THE CONTROL CRACK LENGTH SPECIFIED IS  2.50000 INCHES

| FLIGHT, | CRACK LENGTH | FLIGHT | CRACK LENGTH |
|---|---|---|---|
| 112 | 0.255822 | 3024 | 0.539010 |
| 224 | 0.261876 | 3136 | 0.559022 |
| 336 | 0.268170 | 3248 | 0.580286 |
| 448 | 0.274720 | 3360 | 0.602912 |
| 560 | 0.281539 | 3472 | 0.627022 |
| 672 | 0.288640 | 3584 | 0.652748 |
| 784 | 0.296040 | 3696 | 0.680406 |
| 896 | 0.303753 | 3808 | 0.710877 |
| 1008 | 0.311798 | 3920 | 0.743715 |
| 1120 | 0.320191 | 4032 | 0.779164 |
| 1232 | 0.328951 | 4144 | 0.816730 |
| 1344 | 0.338097 | 4256 | 0.857096 |
| 1456 | 0.347649 | 4368 | 0.900999 |
| 1568 | 0.357626 | 4480 | 0.948998 |
| 1680 | 0.367950 | 4592 | 1.001791 |
| 1792 | 0.378687 | 4704 | 1.060306 |
| 1904 | 0.389917 | 4816 | 1.125755 |
| 2016 | 0.401674 | 4928 | 1.200252 |
| 2128 | 0.413996 | 5040 | 1.286780 |
| 2240 | 0.426925 | 5152 | 1.390233 |
| 2352 | 0.440508 | 5264 | 1.520556 |
| 2464 | 0.454793 | 5376 | 1.694715 |
| 2576 | 0.469838 | 5488 | 1.955370 |
| 2688 | 0.485704 | 5600 | 2.375599 |
| 2800 | 0.502460 | 5623 | 2.501473 |
| 2912 | 0.520181 | | |

PROGRAM P6 CRACK GROWTH IN 7075 T6 PANELS

FOR THIS SET OF CONDITIONS,

THE NUMBER OF FLIGHTS TAKEN IS 3468

THE CRACK LENGTH REACHED IS 1.35107 INCHES

THE CONTROL CRACK LENGTH SPECIFIED IS 1.35000 INCHES

| FLIGHT, | CRACK LENGTH | FLIGHT | CRACK LENGTH |
|---|---|---|---|
| 69 | 0.255165 | 1863 | 0.486235 |
| 138 | 0.260501 | 1932 | 0.501256 |
| 207 | 0.266019 | 2001 | 0.517029 |
| 276 | 0.271725 | 2070 | 0.533614 |
| 345 | 0.277630 | 2139 | 0.551071 |
| 414 | 0.283744 | 2208 | 0.569380 |
| 483 | 0.290079 | 2277 | 0.588517 |
| 552 | 0.296645 | 2346 | 0.608720 |
| 621 | 0.303454 | 2415 | 0.630103 |
| 690 | 0.310519 | 2484 | 0.652798 |
| 759 | 0.317854 | 2553 | 0.677045 |
| 828 | 0.325472 | 2622 | 0.704036 |
| 897 | 0.333389 | 2691 | 0.733149 |
| 966 | 0.341621 | 2760 | 0.764688 |
| 1035 | 0.350184 | 2829 | 0.798892 |
| 1104 | 0.359097 | 2898 | 0.835951 |
| 1173 | 0.368366 | 2967 | 0.876334 |
| 1242 | 0.378015 | 3036 | 0.920221 |
| 1311 | 0.388075 | 3105 | 0.968262 |
| 1380 | 0.398552 | 3174 | 1.021718 |
| 1449 | 0.409481 | 3243 | 1.082657 |
| 1518 | 0.420880 | 3312 | 1.152640 |
| 1587 | 0.432784 | 3381 | 1.233812 |
| 1656 | 0.445234 | 3450 | 1.325417 |
| 1725 | 0.458267 | 3468 | 1.351066 |
| 1794 | 0.471920 | | |

PROGRAM P7 CRACK GROWTH IN 7075 T6 PANELS

FOR THIS SET OF CONDITIONS,

THE NUMBER OF FLIGHTS TAKEN IS 3679

THE CRACK LENGTH REACHED IS 1.35056 INCHES

THE CONTROL CRACK LENGTH SPECIFIED IS 1.35000 INCHES

| FLIGHT, | CRACK LENGTH | FLIGHT | CRACK LENGTH |
|---|---|---|---|
| 73 | 0.255282 | 1971 | 0.493373 |
| 146 | 0.260742 | 2044 | 0.509094 |
| 219 | 0.266389 | 2117 | 0.525624 |
| 292 | 0.272221 | 2190 | 0.543045 |
| 365 | 0.278250 | 2263 | 0.561391 |
| 438 | 0.284494 | 2336 | 0.580549 |
| 511 | 0.290965 | 2409 | 0.600725 |
| 584 | 0.297675 | 2482 | 0.622031 |
| 657 | 0.304635 | 2555 | 0.644567 |
| 730 | 0.311861 | 2628 | 0.668445 |
| 803 | 0.319365 | 2701 | 0.694454 |
| 876 | 0.327163 | 2774 | 0.722489 |
| 949 | 0.335270 | 2847 | 0.752536 |
| 1022 | 0.343705 | 2920 | 0.784868 |
| 1095 | 0.352486 | 2993 | 0.819419 |
| 1168 | 0.361630 | 3066 | 0.856543 |
| 1241 | 0.371141 | 3139 | 0.896477 |
| 1314 | 0.381056 | 3212 | 0.939160 |
| 1387 | 0.391403 | 3285 | 0.985526 |
| 1460 | 0.402180 | 3358 | 1.036569 |
| 1533 | 0.413441 | 3431 | 1.093784 |
| 1606 | 0.425254 | 3504 | 1.158316 |
| 1679 | 0.437621 | 3577 | 1.231971 |
| 1752 | 0.450578 | 3650 | 1.314918 |
| 1925 | 0.464161 | 3679 | 1.350557 |
| 1998 | 0.478411 | | |